We are IntechOpen, the world's leading publisher of Open Access books Built by scientists, for scientists

4,800
Open access books available

122,000
International authors and editors

135M
Downloads

Our authors are among the

154
Countries delivered to

TOP 1%
most cited scientists

12.2%
Contributors from top 500 universities

CLARIVATE ANALYTICS BOOK CITATION INDEX INDEXED

WEB OF SCIENCE™

Selection of our books indexed in the Book Citation Index in Web of Science™ Core Collection (BKCI)

Interested in publishing with us?
Contact book.department@intechopen.com

Numbers displayed above are based on latest data collected.
For more information visit www.intechopen.com

18

New Approaches for Theoretical Estimation of Mass Transfer Parameters in Both Gas-Liquid and Slurry Bubble Columns

Stoyan NEDELTCHEV and Adrian SCHUMPE
Institute of Technical Chemistry, TU Braunschweig
Germany

1. Introduction

Bubble columns (with and without suspended solids) have been used widely as chemical reactors, bioreactors and equipment for waste water treatment. The key design parameters in bubble columns are:

- gas holdup;
- gas-liquid interfacial area;
- volumetric liquid-phase mass transfer coefficient;
- gas and liquid axial dispersion coefficients;

Despite the large amount of studies devoted to hydrodynamics and mass transfer in bubble columns, these topics are still far from being exhausted. One of the essential reasons for hitherto unsuccessful modeling of hydrodynamics and mass transfer in bubble columns is the unfeasibility of a unified approach to different types of liquids. A diverse approach is thus advisable to different groups of gas-liquid systems according to the nature of liquid phase used (pure liquids, aqueous or non-aqueous solutions of organic or inorganic substances, non-Newtonian fluids and their solutions) and according to the extent of bubble coalescence in the respective classes of liquids. It is also necessary to distinguish consistently between the individual regimes of bubbling pertinent to a given gas-liquid system and to conditions of the reactor performance.

The mechanism of mass transfer is quite complicated. Except for the standard air-water system, no hydrodynamic or mass transfer characteristics of bubble beds can be reliably predicted or correlated at the present time. Both the interfacial area a and the volumetric liquid-phase mass transfer coefficient k_La are considered the most important design parameters and bubble columns exhibit improved values of these parameters (Wilkinson et al., 1992). For the design of a bubble column as a reactor, accurate data about bubble size distribution and hydrodynamics in bubble columns, mechanism of bubble coalescence and breakup as well as mass transfer from individual bubbles are necessary. Due to the complex nature of gas-liquid dispersion systems, the relations between the phenomena of bubble coalescence and breakup in bubble swarms and pertinent fundamental hydrodynamic parameters of bubble beds are still not thoroughly understood.

The amount of gas transferred from bubbles into the liquid phase is determined by the magnitude of k_La. This coefficient is an important parameter and its knowledge is essential

for the determination of the overall rate of chemical reaction in heterogeneous systems, i.e. for the evaluation of the effect of mass transport on the overall reaction rate. The rate of interfacial mass transfer depends primarily on the size of bubbles in the systems. The bubble size influences significantly the value of the mass transfer coefficient k_L. It is worth noting that the effects of so-called tiny bubbles (d_s<0.002 m) and large bubbles (d_s≥0.002 m) are opposite. In the case of tiny bubbles, values of mass transfer coefficient increase rapidly as the bubble size increases. In the region of large bubbles, values of mass transfer coefficient decrease slightly as the bubble diameter increases. However, such conclusions have to be employed with caution. For the sake of correctness, it would therefore be necessary to distinguish strictly between categories of tiny and large bubbles with respect to the type of liquid phase used (e.g. pure liquids or solutions) and then to consider separately the values of liquid-phase mass transfer coefficient k_L for tiny bubbles (with immobile interface), for large bubbles in pure liquids (mobile interface) and for large bubbles in solutions (limited interface mobility).

The axial dispersion model has been extensively used for estimation of axial dispersion coefficients and for bubble column design. Some reliable correlations for the prediction of these parameters have been established in the case of pure liquids at atmospheric pressure. Yet, the estimations of the design parameters are rather difficult for bubble columns with liquid mixtures and aqueous solutions of surface active substances.

Few sentences about the effect of high pressure should be mentioned. Hikita et al. (1980), Öztürk et al. (1987) and Idogawa et al. (1985a, b) in their gas holdup experiments at high pressure observed that gas holdup increases as the gas density increases. Wilkinson et al. (1994) have shown that gas holdup, k_La and a increase with pressure. For design purposes, they have developed their own correlation which relates well k_La and gas holdup. As the pressure increases, the gas holdup increases and the bubble size decreases which leads to higher interfacial area. Due to this reason, Wilkinson et al. (1992) argue that both a and k_La will be underestimated by the published empirical equations. The authors suggest that the accurate estimation of both parameters requires experiments at high pressure. They proposed a procedure for estimation of these parameters on the basis of atmospheric results. It shows that the volumetric liquid-phase mass transfer coefficient increases with pressure regardless of the fact that a small decrease of the liquid-side mass transfer coefficient is expected. Calderbank and Moo-Young (1961) have shown that the liquid-side mass transfer coefficient decreases for smaller bubble size. The increase in interfacial area with increasing pressure depends partly on the relative extent to which the gas holdup increases with increasing pressure and partly on the decrease in bubble size with increasing pressure.

The above-mentioned key parameters are affected pretty much by the bubble size distribution. In turn, it is controlled by both bubble coalescence and breakup which are affected by the physico-chemical properties of the solutions used. On the basis of dynamic gas disengagement experiments, Krishna et al. (1991) have confirmed that in the heterogeneous (churn-turbulent) flow regime a bimodal bubble size distribution exists: small bubbles of average size 5×10^{-3} m and fast rising large bubbles of size 5×10^{-2} m. Wilkinson et al. (1992) have proposed another set of correlations by using gas holdup data obtained at pressures between 0.1 and 2 MPa and extensive literature data.

The flow patterns affect also the values of the above-mentioned parameters. Three different flow regimes are observed:

- homogeneous (bubbly flow) regime;
- transition regime;

- heterogeneous (churn-turbulent) regime.

Under common working conditions of bubble bed reactors, bubbles pass through the bed in swarms. Kastanek et al. (1993) argue that the character of two-phase flow is strongly influenced by local values of the relative velocity between the dispersed and the continuous phase. On the basis of particle image velocimetry (PIV), Chen et al. (1994) observed three flow regimes: a dispersed bubble regime (homogeneous flow regime), vortical-spiral flow regime and turbulent (heterogeneous) flow regime. In the latter increased bubble-wake interactions are observed which cause increased bubble velocity. The vortical-spiral flow regime is observed at superficial gas velocity u_G=0.021-0.049 m/s and is composed of four flow regions (the central plume region, the fast bubble flow region, the vortical-spiral flow region and the descending flow region) from the column axis to the column wall. According to Koide (1996) the vortical-spiral flow region might occur in the transition regime provided that the hole diameter of the gas distributor is small. Chen et al. (1994) have observed that in the fast bubble flow regime, clusters of bubbles or coalesced bubbles move upwards in a spiral manner with high velocity. The authors found that these bubble streams isolate the central plume region from direct mass exchange with the vortical-spiral flow region. In the heterogeneous flow regime, the liquid circulating flow is induced by uneven distribution of gas holdup. At low pressure in the churn-turbulent regime a much wider range of bubble sizes occurs as compared to high pressure. At low pressure there are large differences in rise velocity which lead to a large residence time distribution of these bubbles. In the churn-turbulent regime, frequent bubble collisions occur.

Deckwer (1992) has proposed a graphical correlation of flow regimes with column diameter and u_G. Another attempt has been made to determine the flow regime boundaries in bubble columns by using u_G vs. gas holdup curve (Koide et al., 1984). The authors recommended that if the product of column diameter and hole size of the distributor is higher than 2×10^{-4} m^2, the flow regime is assumed to be a heterogeneous flow regime. In the bubble column with solid suspensions, solid particles tend to induce bubble coalescence, so the homogeneous regime is rarely observed. The transition regime or the heterogeneous regime is usually observed.

In some works on mass transfer, the effects of turbulence induced by bubbles are considered. The flow patterns of liquid and bubbles are dynamic in nature. The time-averaged values of liquid velocity and gas holdup reveal that the liquid rises upwards and the gas holdup becomes larger in the center of the column.

Wilkinson et al. (1992) concluded also that the flow regime transition is a function of gas density. The formation of large bubbles can be delayed to a higher value of superficial gas velocity (and gas holdup) when the coalescence rate is reduced by the addition of an electrolyte. Wilkinson and Van Dierendonck (1990) have demonstrated that a higher gas density increases the rate of bubble breakup especially for large bubbles. As a result, at high pressure mainly small bubbles occur in the homogeneous regime, until for very high gas holdup the transition to the churn-turbulent regime occurs because coalescence then becomes so important that larger bubbles are formed. The dependence of both gas holdup and the transition velocity in a bubble column on pressure can be attributed to the influence of gas density on bubble breakup. Wilkinson et al. (1992) argue that many (very) large bubbles occur especially in bubble columns with high-viscosity liquids. Due to the high rise velocity of the large bubbles, the gas holdup in viscous liquids is expected to be low, whereas the transition to the churn-turbulent regime (due to the formation of large bubbles) occurs at very low gas velocity. The value of surface tension also has a pronounced

influence on bubble breakup and thus gas holdup. When the surface tension is lower, fewer large bubbles occur because the surface tension forces oppose deformation and bubble breakup (Otake et al., 1977). Consequently, the occurrence of large bubbles is minimal due to bubble breakup especially in those liquids that are characterized with a low surface tension and a low liquid viscosity. As a result, relatively high gas holdup values are to be expected for such liquids, whereas the transition to the churn-turbulent regime due to the formation of large bubbles is delayed to relatively high gas holdup values.

1.1 Estimation of bubble size

The determination of the Sauter-mean bubble diameter d_s is of primary importance as its value directly determines the magnitude of the specific interfacial area related to unit volume of the bed. All commonly recommended methods for bubble size measurement yield reliable results only in bubble beds with small porosity (gas holdup≤0.06). The formation of small bubbles can be expected in units with porous plate or ejector type gas distributors. At these conditions, no bubble interference occurs. The distributions of bubble sizes yielded by different methods differ appreciably due to the different weight given to the occurrence of tiny bubbles. It is worth noting that the bubble formation at the orifice is governed only by the inertial forces. Under homogeneous bubbling conditions the bubble population in pure liquids is formed by isolated mutually non-interfering bubbles.

The size of the bubbles leaving the gas distributor is not generally equal to the size of the bubbles in the bed. The difference depends on the extent of bubbles coalescence and break-up in the region above the gas distributor, on the distributor type and geometry, on the distance of the measuring point from the distributor and last but not least on the regime of bubbling. In coalescence promoting systems, the distribution of bubble sizes in the bed is influenced particularly by the large fraction of so-called equilibrium bubbles. The latter are formed in high porosity beds as a result of mutual interference of dynamic forces in the turbulent medium and surface tension forces, which can be characterized by the Weber number We. Above a certain critical value of We, the bubble becomes unstable and splits to bubbles of equilibrium size. On the other hand, if the primary bubbles formed by the distributor are smaller than the equilibrium size, they can reach in turbulent bubble beds the equilibrium size due to mutual collisions and subsequent coalescence. As a result, the mean diameter of bubbles in the bed again approaches the equilibrium value. In systems with suppressed coalescence, if the primary bubble has larger diameter than the equilibrium size, it can reach the equilibrium size due to the break-up process. If however the bubbles formed by the distributor are smaller than the equilibrium ones the average bubble size will remain smaller than the hypothetical equilibrium size as no coalescence occurs. Kastanek et al. (1993) argue that in the case of homogeneous regime the Sauter-mean bubble diameter d_s increases with superficial gas velocity u_G.

The correct estimation of bubble size is a key step for predicting successfully the mass transfer coefficients. Bubble diameters have been measured by photographic method, electroresistivity method, optical-fiber method and the chemical-absorption method. Recently, Jiang et al. (1995) applied the PIV technique to obtain bubble properties such as size and shape in a bubble column operated at high pressures.

In the homogeneous flow regime (where no bubble coalescence and breakup occur), bubble diameters can be estimated by the existing correlations for bubble diameters generated from perforated plates (Tadaki and Maeda, 1963; Koide et al., 1966; Miyahara and Hayashi, 1995)

or porous plates (Hayashi et al., 1975). Additional correlations for bubble size were developed by Hughmark (1967), Akita and Yoshida (1974) and Wilkinson et al. (1994). The latter developed their correlation based on data obtained by the photographic method in a bubble column operated between 0.1-1.5 MPa and with water and organic liquids. In electrolyte solutions, the bubble size is generally much smaller than in pure liquids (Wilkinson et al., 1992).

In the transition regime and the heterogeneous flow regime (where bubble coalescence and breakup occur) the observed bubble diameters exhibit different values depending on the measuring methods. It is worth noting that the volume-surface mean diameter of bubbles measured near the column wall by the photographic method (Ueyama et al., 1980) agrees well with the predicted values from the correlation of Akita and Yoshida (1974). However, they are much smaller than those measured with the electroresistivity method and averaged over the cross-section by Ueyama et al. (1980).

When a bubble column is operated at high pressures, the bubble breakup is accelerated due to increasing gas density (Wilkinson et al., 1990), and so bubble sizes decrease (Idogawa et al., 1985a, b; Wilkinson et al., 1994). Jiang et al. (1995) measured bubble sizes by the PIV technique in a bubble column operated at pressures up to 21 MPa and have shown that the bubble size decreases and the bubble size distribution narrows with increasing pressure. However, the pressure effect on the bubble size is not significant when the pressure is higher than 1.5 MPa.

The addition of solid particles to liquid increases bubble coalescence and so bubble size. Fukuma et al. (1987a) measured bubble sizes and rising velocities using an electro-resistivity probe and showed that the mean bubble size becomes largest at a particle diameter of about 0.2×10^{-3} m for an air-water system. The authors derived also a correlation.

For pure, coalescence promoting liquids, Akita and Yoshida (1974) proposed an empirical relation for bubble size estimation based on experimental data from a bubble column equipped with perforated distributing plates. The authors argue that their equation is valid up to superficial gas velocities of 0.07 m/s. It is worth noting that Akita and Yoshida (1974) used a photographic method which is not very reliable at high gas velocities. The equation does not include the orifice diameter as an independent variable, albeit even in the homogeneous bubbling region this parameter cannot be neglected.

For porous plates and coalescence suppressing media Koide and co-workers (1968) derived their own correlation. However, the application of this correlation requires exact knowledge of the distributor porosity. Such information can be obtained only for porous plates produced by special methods (e.g. electro-erosion), which are of little practical use, while they are not available for commonly used sintered-glass or metal plates. Kastanek et al. (1993) reported a significant effect of electrolyte addition on the decrease of bubble size. According to these authors, for the inviscid, coalescence-supporting liquids the ratio of Sauter-mean bubble diameter to the arithmetic mean bubble diameter is approximately constant (and equal to 1.07) within orifice Reynolds numbers in the range of 200-600. It is worth noting that above a certain viscosity value (higher than 2 mPa s) its further increase results in the simultaneous presence of both large and extremely small bubbles in the bed. Under such conditions the character of bubble bed corresponds to that observed for inviscid liquids under turbulent bubbling conditions. In such cases, only the Sauter-mean bubble diameter should be used for accurate bubble size characteristics. Kastanek et al. (1993) developed their own correlation (valid for orifice Reynolds numbers in between 200 and 1000) for the prediction of Sauter-mean bubble diameter in coalescence-supporting systems.

According to it, the bubble size depends on the volumetric gas flow rate related to a single orifice, the surface tension and liquid viscosity.
The addition of a surface active substance causes the decrease of Sauter-mean bubble diameter to a certain limiting value which then remains unchanged with further increase of the concentration of the surface active agent. It is frequently assumed that the addition of surface active agents causes damping of turbulence in the vicinity of the interface and suppression of the coalescence of mutually contacting bubbles. It is well-known fact that the Sauter-mean bubble diameters corresponding to individual coalescent systems differ only slightly under turbulent bubbling conditions and can be approximated by the interval $6\text{-}7\times10^{-3}$ m.

1.2 Estimation of gas holdup

Gas holdup is usually expressed as a ratio of gas volume V_G to the overall volume (V_G+V_L). It is one of the most important parameters characterizing bubble bed hydrodynamics. The value of gas holdup determines the fraction of gas in the bubble bed and thus the residence time of phases in the bed. In combination with the bubble size distribution, the gas holdup values determine the extent of interfacial area and thus the rate of interfacial mass transfer. Under high gas flow rate, gas holdup is strongly inhomogeneous near the gas distributor (Kiambi et al., 2001).
Gas holdup correlations in the homogeneous flow regime have been proposed by Marrucci (1965) and Koide et al. (1966). The latter is applicable to both homogeneous and transition regimes. It is worth noting that the predictions of both equations agree with each other very well. Correlations for gas holdup in the transition regime are proposed by Koide et al. (1984) and Tsuchiya and Nakanishi (1992). Hughmark (1967), Akita and Yoshida (1973) and Hikita et al. (1980) derived gas holdup correlations for the heterogeneous flow regime. The effects of alcohols on gas holdup were discussed and the correlations for gas holdups were obtained by Akita (1987a) and Salvacion et al. (1995). Koide et al. (1984) argues that the addition of inorganic electrolyte to water increases the gas holdup by 20-30 % in a bubble column with a perforated plate as a gas distributor. Akita (1987a) has reported that no increase in gas holdup is recognized when a perforated plate of similar performance to that of a single nozzle is used. Öztürk et al. (1987) measured gas holdups in various organic liquids in a bubble column, and have reported that gas holdup data except those for mixed liquids with frothing ability are described well by the correlations of Akita and Yoshida (1973) and Hikita et al. (1980). Schumpe and Deckwer (1987) proposed correlations for both heterogeneous flow regime and slug flow regime in viscous media including non-Newtonian liquids. Addition of a surface active substance (such as alcohol) to water inhibits bubble coalescence and results in an increase of gas holdup. Grund et al. (1992) applied the gas disengagement technique for measuring the gas holdup of both small and large bubble classes. Tap water and organic liquids were used. The authors have shown that the contribution of small class bubbles to k_La is very large, e.g. about 68 % at u_G=0.15 m/s in an air-water system. Grund et al. (1992) suggested that a rigorous reactor model should consider two bubble classes with different degrees of depletion of transport component in the gas phase. Muller and Davidson (1992) have shown that small-class bubbles contribute 20-50 % of the gas-liquid mass transfer in a column with highly viscous liquid. Addition of solid particles to liquid in a bubble column reduces the gas holdup and correlations of gas holdup valid for transition and heterogeneous flow regimes were proposed by Koide et al. (1984), Sauer and Hempel (1987) and Salvacion et al. (1995).

Wilkinson et al. (1992) have summarized some of the most important gas holdup correlations and have discussed the role of gas density. The authors reported also that at high pressure gas holdup is higher (especially for liquids of low viscosity) while the average bubble size is smaller. Wilkinson et al. (1992) determined the influence of column dimensions on gas holdup. Kastanek et al. (1993) reported that at atmospheric pressure the gas holdup is virtually independent of the column diameter provided that its value is larger than 0.15 m. This information is critical to scale-up because it determines the minimum scale at which pilot-plant experiments can be implemented to estimate the gas holdup (and mass transfer) in a large industrial bubble column. Wilkinson et al. (1992) reached this conclusion for both low and high pressures and in different liquids.

Wilkinson et al. (1992) argues that the gas holdup in a bubble column is usually not uniform. In general, three regions of different gas holdup are recognized. At the top of the column, there is often foam structure with a relatively high gas holdup, while the gas holdup near the sparger is sometimes measured to be higher (for porous plate spargers) and sometimes lower (for single-nozzle spargers) than in the main central part of the column. The authors argue that if the bubble column is very high, then the gas holdup near the sparger and in the foam region at the top of the column has little influence on the overall gas holdup, while the influence can be significant for low bubble columns. The column height can influence the value of the gas holdup due to the fact that liquid circulation patterns (that tend to decrease the gas holdup) are not fully developed in short bubble columns (bed aspect ratio<3). All mentioned factors tend to cause a decrease in gas holdup with increasing column height. Kastanek et al. (1993) argues that this influence is negligible for column heights greater than 1-3 m and with height to diameter ratios above 5.

Wilkinson et al. (1992) have shown that the influence of the sparger design on gas holdup is negligible (at various pressures) provided the sparger hole diameters are larger than approximately $1\text{-}2\times10^{-3}$ m (and there is no maldistribution at the sparger). In high bubble columns, the influence of sparger usually diminishes due to the ongoing process of bubble coalescence. Wilkinson et al. (1992) argue that the relatively high gas holdup and mass transfer rate that can occur in small bubble columns as a result of the use of small sparger holes will not occur as noticeably in a high bubble column. In other words, a scale-up procedure, in which the gas holdup, the volumetric mass transfer coefficient and the interfacial area are estimated on the basis of experimental data obtained in a pilot-plant bubble column with small dimensions (bed aspect ratio<5, D_c<0.15 m) or with porous plate spargers, will in general lead to a considerable overestimation of these parameters. Shah et al. (1982) reported many gas holdup correlations developed on the basis of atmospheric data and they do not incorporate any influence of gas density.

In the case of liquid mixtures, Bach and Pilhofer (1978), Godbole et al. (1982) and Khare and Joshi (1990) determined that gas holdup does not decrease if the viscosity of water is increased by adding glycerol, carboxymethyl cellulose (CMC) or glucose but passes through a maximum. Wilkinson et al. (1992) assumes that this initial increase in gas holdup is due to the fact that the coalescence rate in mixtures is lower than in pure liquids. The addition of an electrolyte to water is known to hinder coalescence with the result that smaller bubbles occur and a higher gas holdup than pure water.

The addition of solids to a bubble column will in general lead to a small decrease in gas holdup (Reilly et al., 1986) and the formation of larger bubbles. The significant increase in gas holdup that occurs in two-phase bubble columns (due to the higher gas density) will also occur in three-phase bubble columns. A temperature increase leads to a higher gas

holdup (Bach and Pilhofer, 1978). A change in temperature can have an influence on gas holdup for a number of reasons: due to the influence of temperature on the physical properties of the liquid, as well as the influence of temperature on the vapor pressure.

Akita and Yoshida (1973) proposed their own correlation for gas holdup estimation. The correlation can be safely employed only within the set of systems used in the author's experiments, i.e. for systems air (O_2, He, CO_2)-water, air-methanol and air-aqueous solutions of glycerol. The experiments were carried out in a bubble column 0.6 m in diameter. The clear liquid height ranged between 1.26 and 3.5 m. It is worth noting that the effect of column diameter was not verified. Hikita and co-workers (1981) proposed another complex empirical relation for gas holdup estimation based on experimental data obtained in a small laboratory column (column diameter=0.1 m, clear liquid height=0.65 m). Large set of gas-liquid systems including air-(H_2, CO_2, CH_4, C_3H_8, N_2)-water, as well as air-aqueous solutions of organic liquids and electrolytes were used. For systems containing pure organic liquids the empirical equation of Bach and Pilhofer (1978) is recommended. The authors performed measurements in the systems air-alcohols and air-halogenated hydrocarbons carried out in laboratory units 0.1-0.15 m in diameter, at clear liquid height > 1.2 m. Hammer and co-workers (1984) proposed an empirical correlation valid for pure organic liquids at low superficial gas velocities. The authors pointed out that there is no any relation in the literature that can express the dependence of gas holdup on the concentration in binary mixtures of organic liquids. The effect of the gas distributor on gas holdup can be important particularly in systems with suppressed bubble coalescence. The majority of relations can be employed only for perforated plate distributors, while considerable increase of gas holdup in coalescence suppressing systems is observed in units with porous distributors. Kastanek et al. (1993) argue that the distributor geometry can influence gas holdup in turbulent bubble beds even in coalescence promoting systems at low values of bed aspect ratio and plate holes diameter.

The gas holdup increases with decreasing surface tension due to the lower rise velocity of bubbles. The effect of surface tension in systems containing pure liquids is however only slight. Gas holdup is strongly influenced by the liquid phase viscosity. However, the effect of this property is rather controversial. The effect of gas phase properties on gas holdup is generally of minor importance and only gas viscosity is usually considered as an important parameter. Large bubble formation leads to a decrease in the gas holdup. Kawase et al. (1987) developed a theoretical correlation for gas holdup estimation. Godbole et al. (1984) proposed a correlation for gas holdup prediction in CMC solutions.

Most of the works in bubble columns dealing with gas holdup measurement and prediction are based on deep bubble beds (Hughmark, 1967; Akita and Yoshida, 1973; Kumar et al., 1976; Hikita et al., 1980; Kelkar et al., 1983; Behkish et al., 2007). A unique work concerned with gas holdup ε_G under homogeneous bubbling conditions was published by Hammer et al. (1984). The authors presented an empirical relation valid for pure organic liquids at $u_G \leq 0.02$ m·s^{-1}. Idogawa et al. (1987) proposed an empirical correlation for gas densities up to 121 kg·m^{-3} and u_G values up to 0.05 m·s^{-1}. Kulkarni et al. (1987) derived a relation to compute ε_G in the homogeneous flow regime in the presence of surface–active agents. By using a large experimental data set, Syeda et al. (2002) have developed a semi–empirical correlation for ε_G prediction in both pure liquids and binary mixtures. Pošarac and Tekić (1987) proposed a reliable empirical correlation which enables the estimation of gas holdup in bubble columns operated with dilute alcohol solutions. A number of gas holdup correlations were summarized by Hikita et al. (1980). Recently, Gandhi et al. (2007) have

proposed a support vector regression–based correlation for prediction of overall gas holdup in bubble columns. As many as 1810 experimental gas holdups measured in various gas–liquid systems were satisfactorily predicted (average absolute relative error: 12.1%). The method is entirely empirical.

In the empirical correlations, different dependencies on the physicochemical properties and operating conditions are implicit. This is primarily because of the limited number of liquids studied and different combinations of dimensionless groups used. For example, the gas holdup correlation proposed by Akita and Yoshida (1973) can be safely employed only within the set of systems used in the authors' experiments (water, methanol and glycerol solutions). The effect of column diameter D_c was not verified and the presence of this parameter in the dimensionless groups is thus only formal. In general, empirical correlations can describe ε_G data only within limited ranges of system properties and working conditions. In this work a new semi–theoretical approach for ε_G prediction is suggested which is expected to be more generally valid.

1.3 Estimation of volumetric liquid-phase mass transfer coefficient

The volumetric liquid-phase mass transfer coefficient is dependent on a number of variables including the superficial gas velocity, the liquid phase properties and the bubble size distribution. The relation for estimation of k_La proposed by Akita and Yoshida (1974) has been usually recommended for a conservative estimate of k_La data in units with perforated-plate distributors. The equation of Hikita and co-workers (1981) can be alternatively employed for both electrolytes and non-electrolytes. However, the reactor diameter was not considered in their relation. Hikita et al. (1981), Hammer et al. (1984) and Merchuk and Ben-Zvi (1992) developed also a correlation for prediction of the volumetric liquid-phase mass transfer coefficient k_La.

Calderbank (1967) reported that values of k_L decrease with increasing apparent viscosity corresponding to the decrease in the bubble rise velocity which prolongs the exposure time of liquid elements at the bubble surface. The k_L value for the frontal area of the bubble is higher than the one predicted by the penetration theory and valid for rigid spherical bubbles in potential flow. The rate of mass transfer per unit area at the rear surface of spherical-cap bubbles in water is of the same order as over their frontal areas. For more viscous liquids, the equation from the penetration theory gives higher values of k_L than the average values observed over the whole bubble surface which suggests that the transfer rate per unit area at the rear of the bubble is less than at its front.

Calderbank (1967) reported that the increase of the pseudoplastic viscosity reduces the rate of mass transfer generally, this effect being most substantial for small bubbles and the rear surfaces of large bubbles. The shape of the rear surface of bubbles is also profoundly affected. Evidently these phenomena are associated with the structure of the bubble wake.

In the case of coalescence promoting liquids, almost no differences have been reported between k_La values determined in systems with large- or small-size bubble population. For coalescence suppressing systems, it is necessary to distinguish between aqueous solutions of inorganic salts and aqueous solutions of surface active substances in which substantial decrease of surface tension occurs. Values of k_La reported in the literature for solutions of inorganic salts under conditions of suppressed bubble coalescence are in general several times higher than those for coalescent systems. On the other hand, k_La values observed in the presence of surface active agents can be higher or lower than those corresponding to

pure water. No quantitative relations are at present available for prediction of k_La in solutions containing small bubbles. The relation of Calderbank and Moo-Young (1961) is considered the best available for the prediction of k_L values. It is valid for bubble sizes greater than 2.5×10^{-3} m and systems water-oxygen, water-CO_2 and aqueous solutions of glycol or polyacrylamide-CO_2. For small bubbles of size less than 2.5×10^{-3} m in systems of aqueous solutions of glycol-CO_2, aqueous solutions of electrolytes-air, waxes-H_2 these authors proposed another correlation. An exhaustive survey of published correlations for k_La and k_L was presented by Shah and coworkers (1982). The authors stressed the important effect of both liquid viscosity and surface tension. Kawase and Moo-Young (1986) proposed also an empirical correlation for k_La prediction. The correlation developed by Nakanoh and Yoshida (1980) is valid for shear-thinning fluids.

In many cases of gas-liquid mass transfer in bubble columns, the liquid-phase resistance to the mass transfer is larger than the gas-phase one. Both the gas holdup and the volumetric liquid-phase mass transfer coefficient k_La increase with gas velocity. The correlations of Hughmark (1967), Akita and Yoshida (1973) and Hikita et al. (1981) predict well k_La values in bubble columns of diameter up to 5.5 m. Öztürk et al. (1987) also proposed correlation for k_La prediction in various organic liquids. Suh et al. (1991) investigated the effects of liquid viscosity, pseudoplasticity and viscoelasticity on k_La in a bubble column and they developed their own correlation. In highly viscous liquids, the rate of bubble coalescence is accelerated and so the values of k_La decrease. Akita (1987a) measured the k_La values in inorganic aqueous solutions and derived their own correlation. Addition of surface-active substances such as alcohols to water increases the gas holdup, however, values of k_La in aqueous solutions of alcohols become larger or smaller than those in water according to the kind and concentration of the alcohol (Salvacion et al., 1995). Akita (1987b) and Salvacion et al. (1995) proposed correlations for k_La prediction in alcohol solutions.

The addition of solid particles (with particle size larger than 10 μm) increases bubble coalescence and bubble size and hence decreases both gas holdup and k_La. For these cases, Koide et al. (1984) and Yasunishi et al. (1986) proposed correlations for k_La prediction. Sauer and Hempel (1987) proposed k_La correlations for bubble columns with suspended particles. Sada et al. (1986) and Schumpe et al. (1987) proposed correlations for k_La prediction in bubble columns with solid particles of diameter less than 10 μm. Sun and Furusaki (1989) proposed a method to estimate k_La when gel particles are used. Sun and Furusaki (1989) and Salvacion et al. (1995) showed that k_La decreases with increasing solid concentration in gel-particle suspended bubble columns. Salvacion et al. (1995) showed that the addition of alcohol to water increases or decreases k_La depending on the kind and concentration of the alcohol added to the water and proposed a correlation for k_La including a parameter of retardation of surface flow on bubbles by the alcohol.

1.4 Estimation of liquid-phase mass transfer coefficient

The liquid-phase mass transfer coefficients k_L are obtained either by measuring k_La, gas holdup and bubble size or by measuring k_La and a with the chemical absorption method. Due to the difficulty in measuring distribution and the averaged value of bubble diameters in a bubble column, predicted values of k_L by existing correlations differ. Hughmark (1967), Akita and Yoshida (1974) and Fukuma et al. (1987b) developed correlations for k_L prediction. In the case of slurry bubble columns, Fukuma et al. (1987b) have shown that the degrees of dependence of k_L on both bubble size and the liquid viscosity are larger than

those in a bubble column. Schumpe et al. (1987) have shown that low concentrations of high density solids of size less than 10 μm increase k_L by a hydrodynamic effect on the liquid film around the bubbles.

For pure liquids and large bubbles ($d_s \geq 0.002$ m), Higbie's (1935) relation based on the penetration theory of mass transfer can be used as the first approximation yielding qualitative information on the effect of fundamental physico-chemical parameters (viscosity, density, surface tension) on k_L values. All these parameters influence both the size of the bubbles (and consequently also their ascending velocity) and the hydrodynamic situation at the interface (represented by an appropriate value of liquid molecular diffusivity). Kastanek et al. (1993) proposed their own correlation for calculation of k_L.

Values of k_L decrease with increasing apparent viscosity corresponding to the decrease in bubble rise velocity which prolongs the exposure time of liquid elements at the bubble surface. According to Calderbank (1967), k_L for the frontal area is 1.13 times higher than the one predicted by the penetration theory and valid for spherical bubbles in potential flow. In the case of water, the rate of mass transfer per unit area at the rear surface of spherical-cap bubbles is of the same order as over their frontal areas. For more viscous liquids, the transfer rate per unit area at the rear of the bubble is less than at its front.

Calderbank (1967) reported that in general the increase of pseudoplastic viscosity reduces the rate of mass transfer, this effect being most substantial for small bubbles and the rear surfaces of large bubbles. The shape of the rear surface of bubbles is also profoundly affected. According to Calderbank (1967), these phenomena are associated with the structure of the bubble wake. Calderbank and Patra (1966) have shown experimentally that the average k_L obtained during the rapid formation of a bubble at a submerged orifice is less than the value observed during its subsequent ascent. According to the authors, this is a consequence of the fact that if the rising bubbles are not in contact with each other the mean exposure time of liquid elements moving round the surface of a rising bubble must be less than the corresponding exposure time during its formation.

Large bubbles ($d_s > 2.5\times10^{-3}$ m) have greater mass transfer coefficients than small bubbles ($d_s < 2.5\times10^{-3}$ m). Small "rigid sphere" bubbles experience friction drag, causing hindered flow in the boundary layer sense. Under these circumstances the mass transfer coefficient is proportional to the two-thirds power of the diffusion coefficient (Calderbank, 1967). For large bubbles ($>2.5\times10^{-3}$ m) form drag predominates and the conditions of unhindered flow envisaged by Higbie (1935) are realized. The author assumed unhindered flow of liquid round the bubble and destruction of concentration gradients in the wake of the bubble.

Griffith (1960) suggested that the mass transfer coefficient for the region outside a bubble may be computed if one knows the average concentration of solute in the liquid outside the bubble, the solute concentration at the interface and the rate of solute transfer. Leonard and Houghton (1963) reported that the k_L values for pure carbon dioxide bubbles dissolving in water is proportional to the square of the instantaneous bubble radius for diameters in the range $6\text{-}11\times10^{-3}$ m where the rise velocity appeared to be independent of size. Leonard and Houghton (1961) found that for bubbles with diameters below 6×10^{-3} m mass transfer seems to have an appreciable effect upon the velocity of rise, indicating that surface effects predominate in this range of sizes. Hammerton and Garner (1954) argue that there is a simple hydrodynamic correspondence between bubble velocity and mass transfer rate. According to Leonard and Houghton (1963) k_L is not only a function of bubble diameter but is also a function of the distance from the point of release. The variation of k_L with distance

from the release point indicates that the rate is a function of time after release or some other related variable such as bubble size or hydrostatic pressure. Baird and Davidson (1962) observed a time dependence for carbon dioxide bubbles in water, but only for bubbles larger than 25×10^{-3} m in diameter, the explanation being that the time dependence was due to the unsteady state eddy diffusion into the turbulent wake at the rear of the bubble. Davies and Taylor (1950) developed a relation for k_L prediction in potential flow around a spherical-cap bubble. The authors argue that the bubble shape becomes oblate spheroidal for bubble sizes below 15×10^{-3} m.

Leonard and Houghton (1963) reported that the effect of inert gas is to reduce somewhat the mass transfer rate by about 20-40 % and to introduce more scatter in the calculated values of k_L, presumably because of the smaller volume changes. Gas circulation is also involved. The effect of an inert gas is to reduce the specific absorption rate, presumably by providing a gas-film resistance that may be affected by internal circulation.

Leonard and Houghton (1963) argue that there is a detectable decrease of k_L with increasing distance from the release point during absorption, the reverse appearing to be true for desorption. The addition of surfactant can reduce mass transfer without affecting the rise velocity. Mass transfer from single rising bubbles is governed to a large extent by surface effects, particularly at the smaller sizes.

The theory of isotropic turbulence can be used also for k_L prediction (Deckwer, 1980). The condition of local isotropy is frequently encountered. The theory of local isotropy gives information on the turbulent intensity in the small volume around the bubble. Turbulent flow produces primary eddies which have a wavelength or scale of similar magnitude to the dimensions of the main flow stream. These large primary eddies are unstable and disintegrate into smaller bubbles until all their energy is dissipated by viscous flow. When the Reynolds number of the main flow is high most of the kinetic energy is contained in the large eddies but nearly all of the dissipation occurs in the smallest eddies. If the scale of the main flow is large in comparison with that of the energy-dissipating eddies a wide spectrum of intermediate eddies exist which contain and dissipate little of the total energy. The large eddies transfer energy to smaller eddies in all directions and the directional nature of the primary eddies is gradually lost. Kolmogoroff (1941) concludes that all eddies which are much smaller than the primary eddies are statistically independent of them and the properties of these small eddies are determined by the local energy dissipation rate per unit mass of fluid. For local isotropic turbulence the smallest eddies are responsible for most of the energy dissipation and their time scale is given by Kolmogoroff (1941). Turbulence in the immediate vicinity of a bubble affects heat and mass transfer rates between the bubble and the liquid and may lead to its breakup.

Kastanek et al. (1993) suggested that the mass transfer in the turbulent bulk-liquid region is accomplished by elementary transfer eddies while in the surface layer adjacent to the interface turbulence is damped and mass transfer occurs due to molecular diffusion. In agreement with the theory of isotropic turbulence, the authors represented the contact time as the ratio of the length of elementary transport eddy to its velocity at the boundary between the bulk liquid and diffusion layer. Kastanek et al. (1993) argue that the rate of mass transfer between the gaseous and the liquid phase is decisively determined by the rate of energy dissipation in the liquid phase.

Kastanek (1977) and Kawase et al. (1987) developed a theoretical model for prediction of volumetric mass transfer coefficient in bubble columns. It is based on Higbie's (1935) penetration theory and Kolmogoroff's theory of isotropic turbulence. It is believed that

turbulence brings up elements of bulk fluid to the free surface where unsteady mass transfer occurs for a short time (called exposure or contact time) after which the element returns to the bulk and is replaced by another one. The exposure time must either be determined experimentally or deduced from physical arguments. Calderbank and Moo-Young (1961) and Kawase et al. (1987) developed a correlation relating the rate of energy dissipation to turbulent mass transfer coefficient at fixed surfaces.

1.5 Estimation of gas-phase mass transfer coefficient

There is a lack of research in the literature on the estimation of the volumetric gas-phase mass transfer coefficients k_Ga. On the basis of chemical absorption and vaporization experiments Metha and Sharma (1966) correlated the k_Ga values to the molecular diffusivity in gas, the superficial gas velocity and static liquid height. Botton et al. (1980) measured k_Ga by the chemical absorption method in a SO_2 (in air)-Na_2CO_3 aqueous solution system in a wide range of u_G values. Cho and Wakao (1988) carried out experiments on stripping of five organic solutes with different Henry's law constants in a batch bubble column with water and they proposed two correlations (for single nozzle and for porous tube spargers) for k_Ga prediction. Sada et al. (1985) developed also correlation for k_Ga prediction. In the case of slurry bubble columns, the authors measured k_Ga by using chemical adsorption of lean CO_2 into NaOH aqueous solutions with suspended $Ca(OH)_2$ particles and they developed a correlation. Its predictions agree well with those observed by Metha and Sharma (1966) and Botton et al. (1980) in a bubble column.

The gas-phase mass transfer coefficient k_G decreases with increasing pressure due to the fact that the gas diffusion coefficient is inversely proportional to pressure (Wilkinson et al., 1992). In the case of bubble columns equipped with single nozzle and porous tube spargers the k_Ga value can be calculated by the correlation of Cho and Wakao (1988).

1.6 Estimation of interfacial area

The specific gas-liquid interfacial area varies significantly when hydrodynamic conditions change. Several methods exist for interfacial area measurements in gas-liquid dispersions. These are photographic, light attenuation, ultrasonic attenuation, double-optical probes and chemical absorption methods. These methods are effective under certain conditions only. For measuring local interfacial areas at high void fractions (more than 20 %) intrusive probes (for instance, double optical probe) are indispensable (Kiambi et al., 2001).

Calderbank (1958) developed a correlation for the specific interfacial area in the case of non-spherical bubbles. Akita and Yoshida (1974) derived also their own empirical equation for the estimation of the interfacial area. Leonard and Houghton (1963) related the interfacial area to the bubble volume using a constant shape factor, which would be 4.84 for spherical bubbles. In the case of perforated plates, Kastanek et al. (1993) reported a correlation for the estimation of the interfacial area. Very frequently the reliability of estimation of the specific interfacial area depends on the accuracy of gas holdup determination.

2. Effect of bubble shape on mass transfer coefficient

Deformed bubbles are generally classified as ellipsoids or spherical caps (Griffith, 1960; Tadaki and Maeda, 1961). The shapes and paths of larger non-spherical bubbles are generally irregular and vary rapidly with time, making the exact theoretical treatment

impossible. Bubbles greater than 1.8×10^{-2} m in diameter assume mushroom-like or spherical-cap shapes and undergo potential flow. Calderbank (1967) argue that the eccentricity decreases with increasing viscosity accompanied by the appearance of "tails" behind small bubbles and of spherical indentations in the rear surfaces.

Calderbank et al. (1970) developed a new theory for mass transfer in the bubble wake. Their work with aqueous solutions of glycerol covers the bubble size range $0.2\text{-}6.0\times10^{-2}$ m and includes the various bubble shapes as determined by the bubble size and the viscosity of the Newtonian liquid. Calderbank and Lochiel (1964) measured the instantaneous mass transfer coefficients in the liquid phase for carbon dioxide bubbles rising through a deep pool of distilled water. Redfield and Houghton (1965) determined mass transfer coefficients for single carbon dioxide bubbles averaged over the whole column using aqueous Newtonian solutions of dextrose. Davenport et al. (1967) measured mass transfer coefficients averaged over column lengths of up to 3 m for single carbon dioxide bubbles in water aqueous solutions of polyvinyl alcohol and ethyl alcohol, respectively. Angelino (1966) has reported some shapes and terminal rise velocities for air bubbles in various Newtonian liquids. Liquid-phase mass transfer coefficients for small bubbles rising in glycerol have been determined by Hammerton and Garner (1954) over bubble diameters ranging from 0.2×10^{-2} m to 0.6×10^{-2} m. Barnett et al. (1966) reported the liquid-phase mass transfer coefficients for small CO_2 bubbles ($0.5\text{-}4.5\times10^{-3}$ m) rising through pseudoplastic Newtonian liquids. This bubble size range was extended to $3\text{-}50\times10^{-3}$ m in the data reported by Calderbank (1967). Astarita and Apuzzo (1965) presented experimental results on the rising velocity and shapes of bubbles in both purely viscous and viscoeleastic non-Newtonian pseudoplastic liquids. According to Calderbank et al. (1970) bubble shapes observed in distilled water vary from spherical to oblate spheroidal ($0.42\text{-}1.81\times10^{-2}$ m) to spherical cap ($1.81\text{-}3.79\times10^{-2}$ m) with increasing bubble size. Over the size range ($4.2\text{-}70\times10^{-3}$ m) the bubbles rise with a zigzag or spiral motion and between bubble diameters of 7×10^{-3} m (Re=1800) and 18×10^{-3} m (Re=5900) an irregular ellipsoid shape is adopted and the bubble pulsates about its mean shape. Over the bubble size range $1.8\text{-}3.0\times10^{-2}$ m a transition from irregular ellipsoid to spherical cap shape occurs and surface rippling is much more evident. For bubble sizes greater than 3×10^{-2} m the bubbles adopt fully developed spherical cap shapes and exhibit little surface rippling. These spherical cap bubbles rise rectilinearly.

Calderbank et al. (1970) developed theory of mass transfer from the rear of spherical-cap bubbles. The authors argue that the overall mass transfer coefficients enhance by hydrodynamic instabilities in the liquid flow round bubbles near the bubble shape transition from spherical cap to oblate spheroid. Calderbank et al. (1970) reported that for bubble sizes $1\text{-}1.8\times10^{-2}$ m a shape transition occurs, the bubble rear surface is gradually flattening and becoming slightly concave as the bubble size is increased. The onset of skirting is accompanied by a flattening of the bubble rear surface. The authors argue that the bubble eccentricity decreases with increasing Newtonian liquid viscosity, though there is a tendency towards convergence at large bubble sizes.

Davidson and Harrison (1963) indicated that the onset of slug flow occurs approximately at bubble size/column diameter>0.33. In the case of spherical-cap bubbles it is expected that there will be appreciable variations between front and rear surfaces. Behind the spherical-cap bubble is formed a torroidal vortex.

Calderbank et al. (1970) reported that a maximum value of k_L occurs shortly before the onset of creeping flow conditions and corresponds to a bubble shape transition from spherical cap to oblate spheroid. This shape transition and the impending flow regime transition results in

instabilities in the liquid flow around the bubble resulting in k_L enhancement. The results of Zieminski and Raymond (1968) indicate that for CO_2 bubbles a maximum of k_L occurs at bubble size of 3×10^{-3} m which they attribute to a progressive transition between circulating and rigid bubble behavior.
Calderbank (1967) stated that the theory of mass transfer has to be modified empirically for dispersion in a non-isotropic turbulent field where dispersion and coalescence take place in different regions. Coalescence is greatly influenced by surfactants, the amount of dispersed phase present, the liquid viscosity and the residence time of bubbles. The existing theories throw little light on problems of mass transfer in bubble wakes and are only helpful in understanding internal circulation within the bubble. The mass-transfer properties of bubble swarms in liquids determine the efficiency and dimensions of the bubble column.
If the viscous or inertial forces do not act equally over the surface of a bubble they may cause it to deform and eventually break. A consequence of these dynamic forces acting unequally over the surface of the bubble is internal circulation of the fluid within the bubble which induces viscous stresses therein. These internal stresses also oppose distortion and breakage.

3. New approach for prediction of gas holdup (Nedeltchev and Schumpe, 2008)

Semi-theoretical approaches to quantitatively predict the gas holdup are much more reliable and accurate than the approaches based on empirical correlations. In order to estimate the mass transfer from bubbles to the surrounding liquid, knowledge of the gas-liquid interfacial area is essential. The specific gas–liquid interfacial area, defined as the surface area available per unit volume of the dispersion, is related to gas holdup ε_G and the Sauter–mean bubble diameter d_s by the following simple relation:

$$a = \frac{6\varepsilon_G}{d_s} \tag{1}$$

Strictly speaking, Eq. (1) (especially the numerical coefficient 6) is valid only for spherical bubbles (Schügerl et al., 1977).
The formula for calculation of the interfacial area depends on the bubble shape. Excellent diagrams for bubble shape determination are available in the books of Clift et al. (1978) and Fan and Tsuchiya (1990) in the form of log–log plots of the bubble Reynolds number Re_B vs. the Eötvös number Eo with due consideration of the Morton number Mo. A comparison among the experimental conditions used in our work and the above–mentioned standard plots reveals that the formed bubbles are no longer spherical but oblate ellipsoidal and follow a zigzag upward path as they rise. Vortex formation in the wake of the bubbles is also observed. The specific interfacial area a of such ellipsoidal bubbles is a function of the number of bubbles N_B, the bubble surface S_B and the total dispersion volume V_{total} (Painmanakul et al., 2005; Nedeltchev et al., 2006a, b, 2007a):

$$a = \frac{N_B S_B}{V_{total}} = \frac{N_B S_B}{AH} \tag{2}$$

where A denotes the column cross–sectional area. The number of bubbles N_B can be deduced from the bubble formation frequency f_B and bubble residence time (Painmanakul et al., 2005):

$$N_{\text{B}} = f_{\text{B}} \frac{H}{u_{\text{B}}} = \frac{Q_{\text{G}}}{V_{\text{B}}} \frac{H}{u_{\text{B}}} \tag{3}$$

where Q_G is the volumetric gas flow rate, u_B is the bubble rise velocity and V_B is the bubble volume. The substitution of Eq. (3) into Eq. (2) yields:

$$a = \frac{f_{\text{B}} S_{\text{B}}}{A u_{\text{B}}} \tag{4}$$

The bubble rise velocity u_B can be estimated from Mendelson's (1967) correlation:

$$u_{\text{B}} = \sqrt{\frac{2\sigma_{\text{L}}}{\rho_{\text{L}} d_{\text{e}}} + \frac{g d_{\text{e}}}{2}} \tag{5}$$

This equation is particularly suitable for the case of ellipsoidal bubbles.
The volume of spherical or ellipsoidal bubbles can be estimated as follows:

$$V_{\text{B}} = \frac{\pi d_{\text{e}}^3}{6} = \frac{4}{3}\pi \left(\frac{l}{2}\right)^2 \frac{h}{2} \tag{6}$$

If some dimensionless correction factor f_c due to the bubble shape differences is introduced, then Eqs. (1) and (4) might be considered equivalent:

$$\frac{6\varepsilon_{\text{G}}}{d_{\text{s}}} = f_{\text{c}} \frac{f_{\text{B}} S_{\text{B}}}{A u_{\text{B}}} \tag{7}$$

Rearrangement of Eq. (7) yields:

$$\varepsilon_{\text{G}} = f_{\text{c}} \frac{d_{\text{s}} f_{\text{B}} S_{\text{B}}}{6 A u_{\text{B}}} \tag{8}$$

The surface S_B of an ellipsoidal bubble can be calculated as follows (Nedeltchev et al., 2006a, b, 2007a):

$$S_{\text{B}} = \pi \frac{l^2}{2} \left[1 + \left(\frac{h}{l}\right)^2 \frac{1}{2e} \ln \frac{(1+e)}{(1-e)} \right] \tag{9}$$

where e is the bubble eccentricity. It can be calculated as follows:

$$e = \sqrt{1 - \left(\frac{h}{l}\right)^2} \tag{9a}$$

An oblate ellipsoidal bubble is characterized by its length l (major axis of the ellipsoid) and its height h (minor axis of the ellipsoid). The ellipsoidal bubble length l and height h can be estimated by the formulas derived by Tadaki and Maeda (1961) and Terasaka et al. (2004):
for 2<Ta<6:

$$l = \frac{d_{\text{e}}}{1.14 Ta^{-0.176}} \tag{10a}$$

$$h = 1.3 d_e Ta^{-0.352} \tag{10b}$$

for 6<Ta<16.5:

$$l = \frac{d_e}{1.36 Ta^{-0.28}} \tag{11a}$$

$$h = 1.85 d_e Ta^{-0.56} \tag{11b}$$

where

$$Ta = Re_B Mo^{0.23} \tag{12}$$

$$Re_B = \frac{d_e u_B \rho_L}{\mu_L} \tag{13}$$

$$Mo = \frac{g \mu_L^4}{\rho_L \sigma_L^3} \tag{14}$$

It is worth noting that the major axis of a rising oblate ellipsoidal bubble is not always horizontally oriented (Yamashita et al., 1979). The same holds for the minor axis of a rising oblate ellipsoidal bubble, i.e. it is not necessarily vertically oriented (Akita and Yoshida, 1974).
Equations (10a)–(14) were used to calculate both l and h values under the operating conditions examined. The Morton number Mo is the ratio of viscosity force to the surface tension force. The Tadaki number Ta characterizes the extent of bubble deformation; the Ta values fell always in one of the ranges specified above. This fact can be regarded as an additional evidence that the bubbles formed under the operating conditions examined are really ellipsoidal.
The above correlations (Equations (10a)–(14)) imply that one needs to know a priori the bubble equivalent diameter d_e. Very often in the literature is assumed that d_e can be approximated by the Sauter–mean bubble diameter d_s. The latter was estimated by means of the correlation of Wilkinson et al. (1994):

$$\left(\frac{g \rho_L d_s^2}{\sigma_L} \right) = 8.8 \left(\frac{u_G \mu_L}{\sigma_L} \right)^{-0.04} \left(\frac{\sigma_L^3 \rho_L}{g \mu_L^4} \right)^{-0.12} \left(\frac{\rho_L}{\rho_G} \right)^{0.22} \tag{15}$$

Equation (15) implies that the bubble size decreases as the superficial gas velocity u_G or the gas density ρ_G (operating pressure P) increase. The calculated d_s values for all liquids examined imply an ellipsoidal shape. Equation (5) along with Eq. (15) (for d_s estimation) was used also to calculate the bubble Reynolds number Re_B (Eq. (13)) needed for the estimation of both l and h values.
The bubble equivalent diameter d_e of an ellipsoidal bubble can be also calculated from Eq. (6) by assuming a sphere of equal volume to the volume of the ellipsoidal bubble:

$$d_e = \left(l^2 h \right)^{1/3} \tag{16}$$

Estimating the characteristic length of ellipsoidal bubbles with the same surface–to–volume ratio (the same d_s value as calculated from Eq. (15)) required an iterative procedure but led to only insignificantly different values than simply identifying the equivalent diameter d_e with d_s when applying Eqs. (10a–b) or (11a–b). In other words, the differences between bubble diameters estimated by Eq. (15) and Eq. (16) are negligibly small.

Liquid	D_c [m]	Gas Sparger	Gases Used	P [MPa]	ρ_L [kg·m^{-3}]	μ_L [10^{-3} Pa·s]	σ_L [10^{-3} N·m^{-1}]
Acetone	0.095	D4	air	0.1	790	0.327	23.1
Anilin	0.095	D4	air	0.1	1022	4.4	43.5
Benzene	0.095	D4	air	0.1	879	0.653	28.7
1–Butanol	0.095 0.102	D1, D2 D4	N_2, air, He	0.1–4.0	809	2.94	24.6
Carbon tetrachloride	0.095	D4	air, He, H_2, CO_2	0.1	1593	0.984	26.1
Cyclohexane	0.095	D4	air	0.1	778	0.977	24.8
Decalin	0.102	D1, D2	N_2, He	0.1–4.0	884	2.66	32.5
1,2-Dichloroethane	0.095	D4	air	0.1	1234	0.82	29.7
1,4-Dioxane	0.095	D4	air	0.1	1033	1.303	32.2
Ethanol (96 %)	0.102	D1, D2, D3	N_2, He	0.1–4.0	793	1.24	22.1
Ethanol (99 %)	0.095	D4	air	0.1	791	1.19	22.1
Ethyl acetate	0.095	D4	air	0.1	900	0.461	23.5
Ethyl benzene	0.095	D4	air	0.1	867	0.669	28.6
Ethylene glycol	0.095 0.102	D1, D2, D4	N_2, air, He	0.1–4.0	1112	19.9	47.7
Gasoline	0.102	D1	N_2	0.1–4.0	692	0.464	21.6
LigroinA (b. p. 90–110 °C)	0.095	D4	air	0.1	714	0.470	20.4
Ligroin B(b. p. 100–140°C)	0.095	D4	air	0.1	729	0.538	21.4
Methanol	0.095	D4	air	0.1	790	0.586	22.2
Nitrobenzene	0.095	D4	air	0.1	1203	2.02	38.1
2–Propanol	0.095	D4	air	0.1	785	2.42	21.1
Tap water	0.095 0.102	D1, D2 D3, D4	N_2, air, He	0.1–4.0	1000	1.01	72.74
Tetralin	0.095	D4	N_2, air, CO_2	0.1	968	2.18	34.9
Toluene	0.095 0.102	D1, D2, D4	N_2, air, He	0.1–4.0	866	0.58	28.5
Xylene	0.095	D4	N_2, air, He, H_2, CO_2	0.1	863	0.63	28.4

Table 1. Properties of the organic liquids and tap water (293.2 K)

Our semi–theoretical approach is focused on the derivation of a correlation for the correction term f_c introduced in Eq. (7). Many liquids covering a large spectrum of physicochemical properties, different gas distributor layouts and different gases at operating pressures up to 4 MPa are considered (Nedeltchev et al., 2007a). As many as 386 experimental gas holdups were obtained in two bubble columns. The first stainless steel column (D_c=0.102 m, H_0=1.3 m) was equipped with three different gas distributors: perforated plate, 19 × Ø 1×10^{-3} m (D1), single hole, 1 × Ø 4.3×10^{-3} m (D2) and single hole, 1 × Ø 1×10^{-3} m (D3) (Jordan and Schumpe, 2001). In the second plexiglass column (D_c=0.095 m, H_0=0.85 m) the gas was always introduced through a single tube of 3×10^{-3} m in ID (D4) (Öztürk et al., 1987). The ε_G values were measured in 21 organic liquids, 17 liquid mixtures and tap water (see Tables 1 and 2).

Liquid Mixture	Key Fig. 9	D_c [m]	Gas Sparger	Gas Used	P [MPa]	ρ_L [kg·m^{-3}]	μ_L [10^{-3} Pa·s]	σ_L [10^{-3} N·m^{-1}]
Benzene/Cyclohexane 6.7 %	A	0.095	D4	air	0.1	865	0.634	27.6
Benzene/Cyclohexane 13.4 %	B	0.095	D4	air	0.1	854	0.628	26.9
Benzene/Cyclohexane 31.5 %	C	0.095	D4	air	0.1	834	0.631	26.2
Benzene/Cyclohexane 54 %	D	0.095	D4	air	0.1	814	0.672	25.4
Benzene/Cyclohexane 78.5 %	E	0.095	D4	air	0.1	797	0.772	24.9
Benzene/Cyclohexane 90 %	F	0.095	D4	air	0.1	787	0.858	24.9
Glycol 22.4 %/Water	G	0.095	D4	air	0.1	1043	2.32	53.8
Glycol 60 %/Water	H	0.095	D4	air	0.1	1072	5.6	52.0
Glycol 80 %/Water	I	0.095	D4	air	0.1	1091	9.65	51.0
Toluene/Ethanol 5 %	J	0.095	D4	air	0.1	863	0.578	27.6
Toluene/Ethanol 13.6 %	K	0.095	D4	air	0.1	859	0.587	27.3
Toluene/Ethanol 28 %	L	0.095	D4	air	0.1	852	0.616	25.5
Toluene/Ethanol 55 %	M	0.095	D4	air	0.1	838	0.731	25.0
Toluene/Ethanol 73.5 %	N	0.095	D4	air	0.1	823	0.961	24.2
Toluene/Ethanol 88.5 %	O	0.095	D4	air	0.1	807	1.013	23.3
Toluene/Ethanol 94.3 %	P	0.095	D4	air	0.1	800	1.103	22.7
Toluene/Ethanol 97.2 %	Q	0.095	D4	air	0.1	796	1.135	22.2

Table 2. Properties of the liquid mixtures (293.2 K)

In both tables are listed the different combinations of liquids, gases, gas distributors and operating pressures that have been used. It is worth noting that in a 0.095 m in ID bubble column equipped with a sparger D4 every liquid or liquid mixture was aerated with air. Table 1 shows that in the case of few liquids (carbon tetrachloride, tetralin, toluene and xylene) some other gases have been used. It should be mentioned that in the case of 0.102 m in ID bubble column no air was used (only nitrogen and helium).

The gas holdups ε_G in 1–butanol, ethanol (96 %), decalin, toluene, gasoline, ethylene glycol and tap water were recorded by means of differential pressure transducers in the 0.102 m stainless steel bubble column operated at pressures up to 4 MPa. The following relationship was used:

$$\varepsilon_{\mathrm{G}} = \frac{\Delta P_{\text{no gas}} - \Delta P_{\text{gas}}}{\Delta P_{\text{no gas}}} \tag{17}$$

where ΔP is the pressure difference between the readings of both lower (at 0 m) and upper (at 1.2 m) pressure transducers. The subscript "no gas" denotes the pressure difference at the clear liquid height H_0, whereas the subscript "gas" denotes the pressure difference at the aerated liquid height H. The gas holdups ε_G in all other liquids and liquid mixtures were estimated by visually observing the dispersion height under ambient pressure in the 0.095 m in ID bubble column. The upper limit (transitional gas velocity) of the homogeneous regime (transition gas velocity u_{trans}) was estimated by the formulas of Reilly et al. (1994).

Most of the gas–liquid systems given in Tables 1 and 2 were characterized with Tadaki numbers Ta lower than 6 and thus Eqs. (10a–b) for the estimation of both bubble length l and bubble height h were applied. Only in the case of ethylene glycol–(helium, air and nitrogen), 1–butanol–(helium and air) and decalin–helium the Ta values exceeded 6 and then Eqs. (11a–b) were used.

It was found that the dimensionless correction factor f_c can be correlated successfully to both the Eötvös number Eo and a dimensionless gas density ratio:

$$f_{\mathrm{c}} = 0.78 Eo^{-0.22}\left(\frac{\rho_{\mathrm{G}}}{\rho_{\mathrm{G}}^{\mathrm{ref}}}\right)^{0.07} = 0.78\left(\frac{g\left(\rho_{\mathrm{L}} - \rho_{\mathrm{G}}\right) d_{\mathrm{e}}^{2}}{\sigma_{\mathrm{L}}}\right)^{-0.22}\left(\frac{\rho_{\mathrm{G}}}{1.2}\right)^{0.07} \tag{18}$$

where ρ_G^{ref} is the reference gas density (1.2 kg·m^{-3} for air at ambient conditions: 293.2 K and 0.1 MPa). All experimental gas holdup data (386 points) were fitted with an average error of 9.6%. The dimensionless gas density ratio is probably needed because the correlation of Wilkinson et al. (1994) was derived for pressures up to 1.5 MPa only, whereas the present data extend up to the pressure of 4 MPa. It is worth noting that Krishna (2000) also used such a dimensionless gas density ratio for correcting his correlations for large bubble rise velocity and dense–phase gas holdup.

Figure 1 illustrates the decrease of the product $f_c(\rho_G/1.2)^{-0.07}$ with increasing Eo. At smaller bubble sizes (with shapes approaching spheres), Eo will be lower and thus f_c higher (gradually approaching unity). It is worth noting that most of the liquids are characterized with Eo values in a narrow range between 2 and 8.

Figure 2 illustrates that the correction factor f_c increases with gas density ρ_G (operating pressure) leading to bubble shrinkage. For example, the correction term f_c decreases in the following sequence: toluene > ethanol > decalin > 1–butanol > ethylene glycol. The smallest bubble size is formed in toluene, whereas the largest bubble size is formed in the case of ethylene glycol. When very small (spherical) bubbles are formed, the correction factor f_c should be equal to unity and both expressions for the interfacial area should become identical (see Eq. (7)).

Figures 3 and 4 exhibit that the experimental gas holdups ε_G measured in 1–butanol, decalin and toluene at pressures up to 4 MPa can be predicted reasonably well irrespective of the gas distributor type.

The same result holds for ethylene glycol and tap water (see Fig. 5). The successful prediction of gas holdups in ethylene glycol should be regarded as one of the most important merits of the presented method since the viscosity is much higher than that of the other liquids.

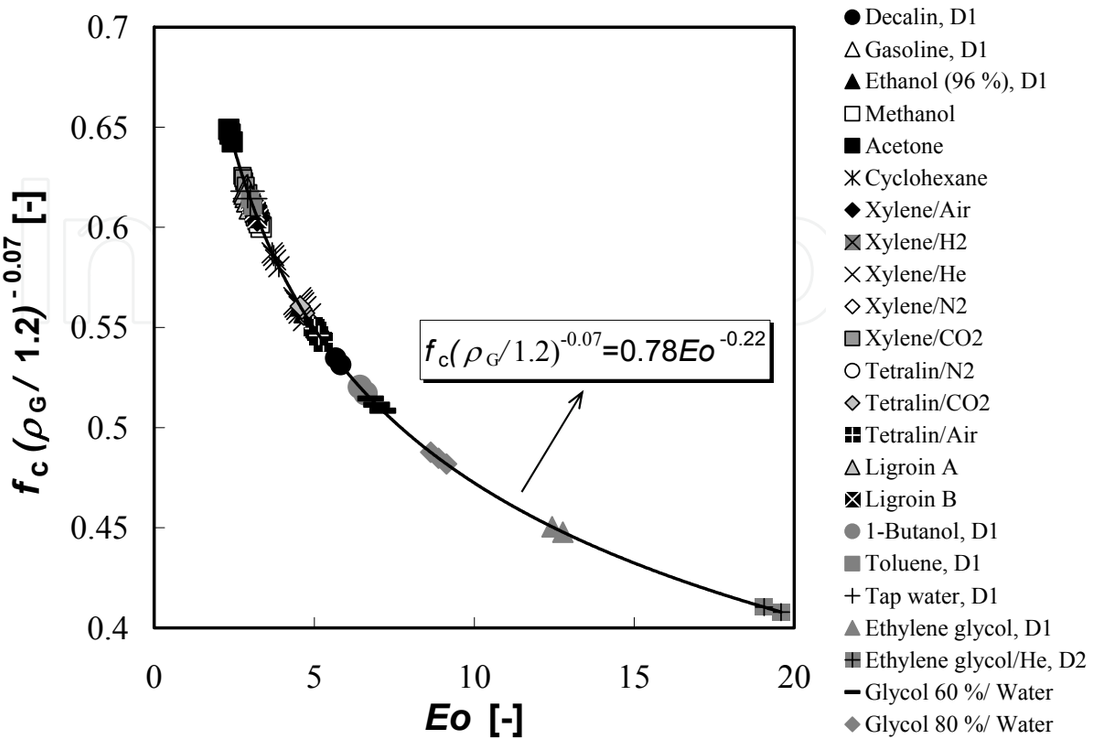

Fig. 1. Product $f_c(\rho_G/1.2)^{-0.07}$ as a function of Eo for 12 organic liquids, 2 liquid mixtures and tap water at ambient pressure (Gas distributor: D4 unless specified in the legend)

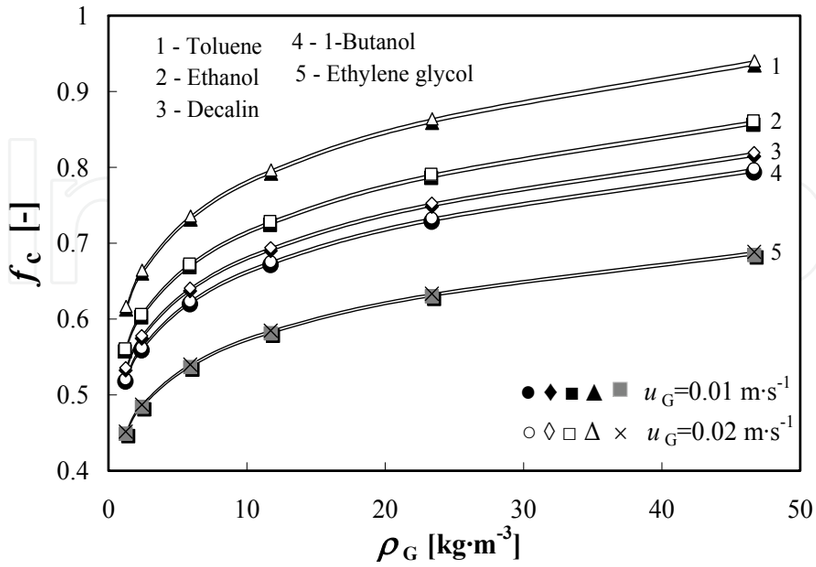

Fig. 2. Correction factor f_c as a function of gas density ρ_G in five organic liquids (Gas distributor: D1; D_c: 0.102 m)

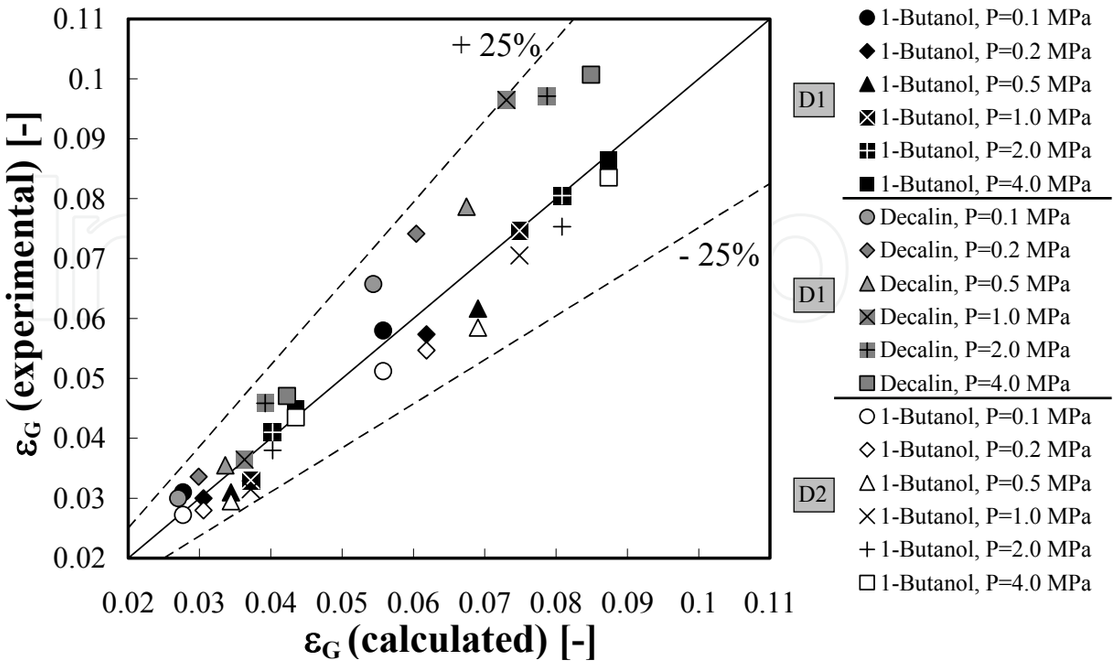

Fig. 3. Parity plot for gas holdups in 1–butanol and decalin sparged with nitrogen through gas distributors D1 and D2 at various pressures

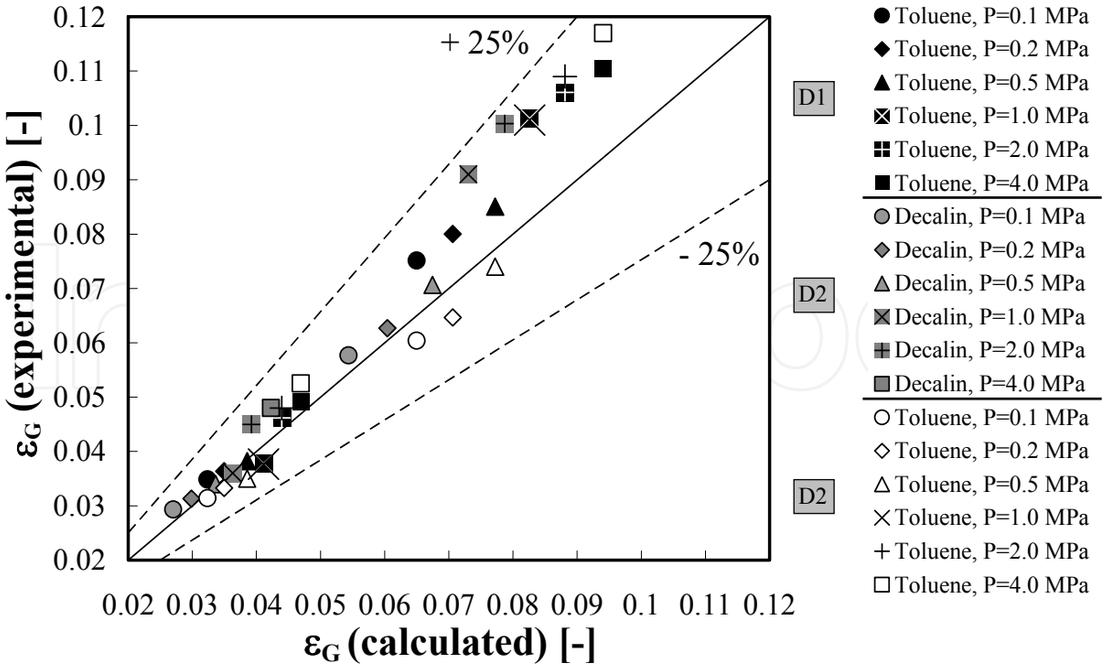

Fig. 4. Parity plot for gas holdups in toluene and decalin sparged with nitrogen through gas distributors D1 and D2 at various pressures

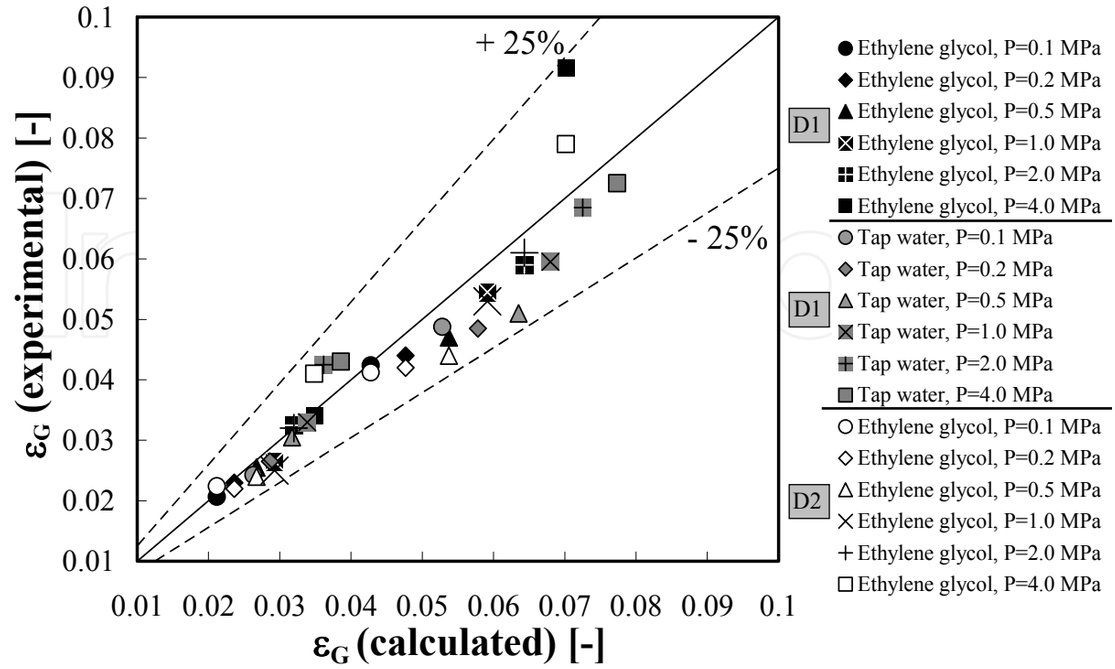

Fig. 5. Parity plot for gas holdups in ethylene glycol and tap water aerated with nitrogen through gas distributors D1 and D2 at various pressures

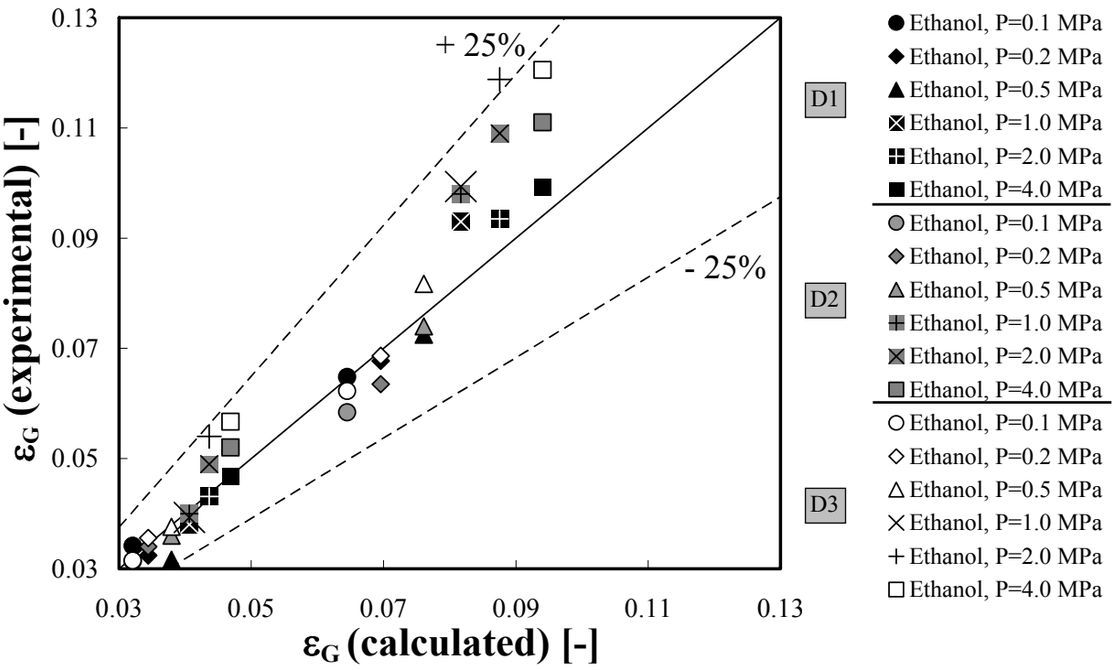

Fig. 6. Parity plot for gas holdups in ethanol (96 %) sparged with nitrogen through gas distributors D1–D3 at various pressures

Figure 6 shows, for ethanol (96 %) as an example, that the gas distributor type is not so important. The same holds for 1–butanol, decalin and toluene (Figs. 3–5) and tap water. This fact is in agreement with the work of Wilkinson et al. (1992) who stated that once the hole size of the gas distributor is greater than 1–2×10^{-3} m, then it has no significant effect on the gas holdup.

Eight organic liquids and tap water have been aerated not only with air or nitrogen but also with other gases (helium, hydrogen and carbon dioxide). Figure 7 shows that the developed model is capable of predicting satisfactorily the experimental gas holdups at these operating conditions.

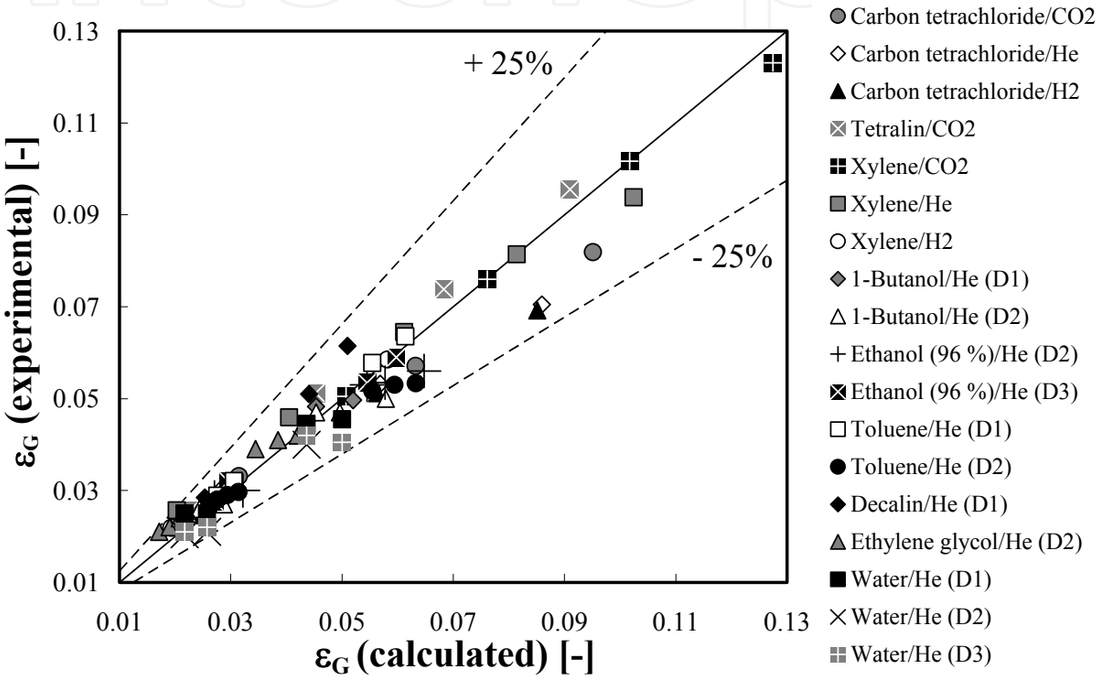

Fig. 7. Parity plot for gas holdups ε_G in 8 organic liquids and tap water aerated with other gases (helium, hydrogen and/or carbon dioxide) at ambient pressure. Gas distributor: D4 unless specified in the legend

Figure 8 shows that the model predicts reasonably well the experimental gas holdups measured in 15 organic liquids at ambient pressure. This fact should be regarded as further evidence that by the introduction of a correction term the presented method becomes generally applicable.

Table 2 and Figs. 3–8 reveal that our approach is applicable not only to tap water but also to organic liquids covering the following ranges of the main physicochemical properties: $692 \le (\rho_L/\text{kg}\cdot\text{m}^{-3}) \le 1593$, $0.327\times10^{-3} \le (\mu_L/\text{Pa}\cdot\text{s}) \le 19.9\times10^{-3}$, $20.4\times10^{-3} \le (\sigma_L/\text{N}\cdot\text{m}^{-1}) \le 47.7\times10^{-3}$.

Figure 9 exhibits that the proposed method for gas holdup prediction along with the new correction factor (Eq. (18)) is also applicable to various liquid mixtures. Table 2 shows that the examined liquid mixtures cover the following ranges of the main physicochemical properties: $787 \le (\rho_L/\text{kg}\cdot\text{m}^{-3}) \le 1091$, $0.578\times10^{-3} \le (\mu_L/\text{Pa}\cdot\text{s}) \le 9.65\times10^{-3}$ and $22.2\times10^{-3} \le (\sigma_L/\text{N}\cdot\text{m}^{-1}) \le 53.8\times10^{-3}$.

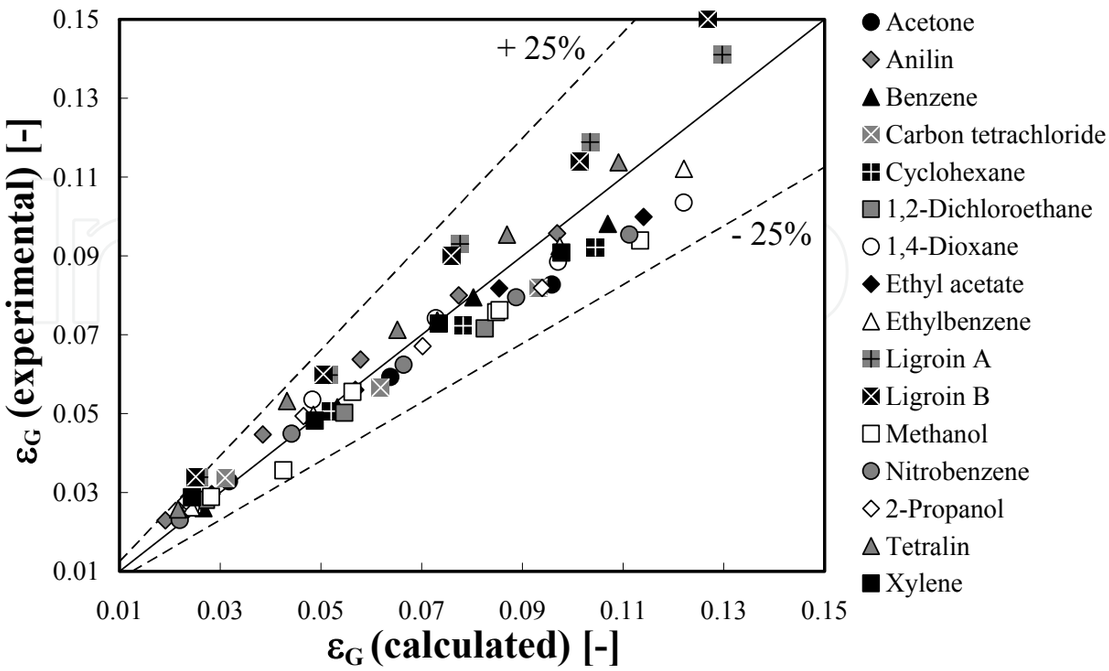

Fig. 8. Parity plot for gas holdups in 15 organic liquids aerated with air by means of gas distributor D4 (D_c=0.095 m) at ambient pressure

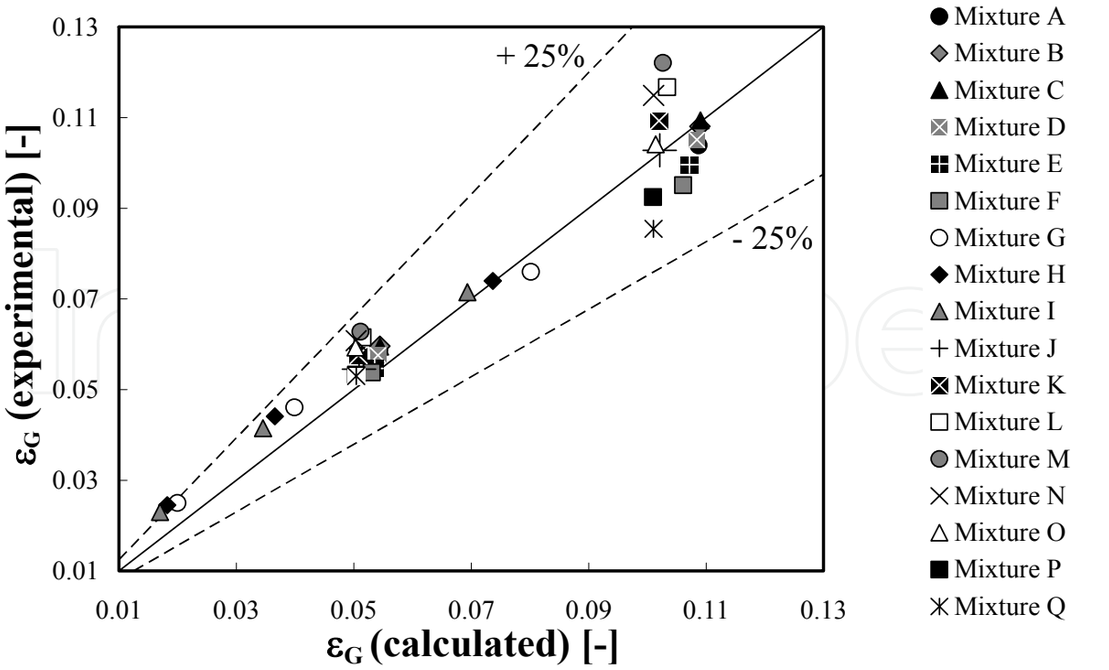

Fig. 9. Parity plot for gas holdups in 17 liquid mixtures sparged with air (gas distributor D4, D_c=0.095 m) at ambient pressure. The legend keys are given in Table 2

Nedeltchev and Schumpe (2008) have shown that in the homogeneous flow regime the semi–theoretical approach improves the gas holdup predictions and turns out to be the most reliable one (since it produces better gas holdup predictions than the empirical correlations of both Hammer et al. (1984) and Akita and Yoshida (1974)). It is worth underlying that our approach is applicable at $u_G \leq u_{trans}$, where the transition gas velocity u_{trans} can be predicted by the correlations of Reilly et al. (1994). In this work, the u_{trans} values were always less than 0.04 $m \cdot s^{-1}$.

4. New approach for prediction of volumetric liquid-phase mass transfer coefficient (Nedeltchev et al., 2006a, b, 2007a)

The k_La value can be predicted if one knows how to estimate both the liquid–side mass transfer coefficient k_L and the interfacial area a. These parameters depend on the bubble diameter. Both k_L and a are closely related to the bubble bed hydrodynamics. k_L incorporates the effects of the complex liquid flow field surrounding the rising gas bubbles. The interfacial area a inherently reflects the system bubble behavior.

Gas bubbles are nonspherical, except when interfacial tension and viscous forces are much more important than inertial forces (Clift et al., 1978). Most of the bubble sizes in this work fall in the range of 1.4–6×10^{-3} m. Such bubbles are no longer spherical and follow a zigzag or helical upward path. Viscous drag is augmented by vortex formation in the wake, and velocity of rise remains fairly constant over the bubble size range (Miller, 1974).

As a rough approximation, Higbie (1935) assumed that the average time of exposure for mass transfer (called contact time or exposure time for mass transfer) can be estimated as follows:

$$t_c = \frac{\text{Bubble surface}}{\text{Rate of surface formation}} \tag{19}$$

In our approach all theoretical k_La calculations were based on this definition of the gas–liquid contact time t_c. The latter characterizes the residence time of the micro eddies (responsible for mass transfer in the liquid film) at the interface, i.e. at the bubble surface. It is practically impossible to measure directly the contact time t_c, so usually it is estimated from correlations for the bubble surface and the rate of surface formation. The contact time is the time required for the bubble to rise through its equivalent spherical diameter. Higbie's (1935) model predicts a decrease in k_L with increase in diameter when in fact it increases quite rapidly. Higbie's theory does not predict an effect of distance from the point of release. The simple model of Higbie (1935) in which the contact time is approximated by macro-scale parameters fails for turbulent bubbling conditions where bubble swarms exist. Higbie's (1935) model assumes direct contact between the gas phase and the bulk liquid.

The contact time takes part in the evaluation of the liquid-phase mass transfer coefficient:

$$k_L = \sqrt{\frac{4D_L}{\pi t_c}} \tag{20}$$

The equation is valid explicitly for rigid spherical bubbles. Higbie (1935) postulated that a gas bubble moving through a liquid splits the liquid at its advancing tip. The penetration theory assumes unsteady–state absorption of a gas by a fluid element adjacent to the surface. The element moves at a uniform velocity from the front of the bubble to the rear as

penetration into it occurs. Timson and Dunn (1960) showed that the bubble surface increases when the spherical bubble is deformed into an ellipsoid. This leads to higher contact time and thus lower k_L value.

In order to calculate the volumetric liquid–side mass transfer coefficient k_La one also needs to know how to calculate the interfacial area a. The formula for its calculation depends on the bubble shape. The specific interfacial area a is a function of the number of bubbles N_B, the bubble surface area S_B and the total dispersion volume V_{total} (see Eq. (2)).

The theoretically calculated k_La values were obtained as a product of both Eq. (20) (using Eq. (19) for the contact time) and Eq. (2). Experimentally, on the other hand, it is much easier to measure the product of k_L and a than the individual values. In the homogeneous flow regime there is a narrow bubble size distribution and the researchers use frequently the Sauter–mean bubble diameter d_s for their mass transfer calculations. The bubbles rise uniformly in nearly straight lines and have roughly uniform bubble size (Krishna, 2000; Lucas et al., 2005). Therefore, it is a reasonable simplification in the homogeneous flow regime to use the mean bubble diameter and disregard the bubble size distribution.

For the sake of theoretical prediction of the k_La values by means of Eqs. (2), (19) and (20) one needs to calculate the bubble surface S_B, the rate of surface formation R_{sf} and the number of bubbles N_B. The calculation of the bubble surface S_B depends on the bubble shape (Painmanakul et al., 2005). Two excellent diagrams for bubble shape determination are available in the books of Clift et al. (1978) and Fan and Tsuchiya (1990) in the form of log–log plots of the bubble Reynolds number Re_B vs. the Eötvös number Eo with due consideration of the Morton number Mo. A comparison among the experimental conditions used in this work and the above–mentioned standard plots reveals that the formed bubbles are no longer spherical but oblate ellipsoidals that follow a zigzag upward path as they rise. Vortex formation in the wake of the bubbles is also observed.

An oblate ellipsoidal bubble is characterized by its length l (major axis of the ellipsoid) and its height h (minor axis of the ellipsoid). The surface area S_B of an ellipsoidal bubble is calculated on the basis of Eqs. (9) and (9a) (Fan and Tsuchiya 1990; Nedeltchev et al., 2006a, b). In order to calculate both ellipsoidal bubble length l and height h, the correlations of Terasaka et al. (2004) (for $2<Ta<6$) were used (see Eqs. (10a-b)). The Tadaki numbers Ta fell always in the range specified above. However, the correlations of Terasaka et al. (2004) imply that one needs to know a priori the bubble equivalent diameter d_e.

Very often in the literature is assumed that d_e can be approximated by the Sauter–mean bubble diameter d_s. Bubble shape, motion and any tendency for the interface to ripple, fluctuate or otherwise deform are all related to bubble size. In turn, bubble size is determined by the physical characteristics of the system and the operating conditions. The d_s value was estimated by means of the correlation of Wilkinson et al. (1994) which is one of the most frequently cited in the literature. This equation implies that the bubble size decreases as superficial gas velocity u_G or gas density ρ_G (operating pressure P) increase. The calculated d_s values for all liquids examined correspond to an ellipsoidal shape.

The bubble equivalent diameter d_e of an ellipsoidal bubble was calculated by assuming a sphere of volume equal to the volume of the ellipsoidal bubble (see Eqs. (6) and (16)). Estimating the characteristic length of ellipsoidal bubbles with the same surface–to–volume ratio (the same d_s value as calculated from Wilkinson et al.'s (1994) correlation) required an iterative procedure but led to only insignificantly different values than simply identifying the equivalent diameter d_e with d_s when applying the correlations for both l and h (see Terasaka et al., 2004).

The equivalent bubble diameter d_e is needed also for the calculation of the bubble rise velocity u_B. The latter was estimated by means of the correlation of Mendelson (1967). This equation is particularly suitable for the case of ellipsoidal bubbles. Mendelson's (1967) correlation for u_B along with Wilkinson et al.'s (1994) relationship for d_s estimation were also used to calculate the bubble Reynolds number Re_B (Eq. (13)) needed for the estimation of both l and h values.
The bubble rise velocity u_B and both the bubble length l and height h of an ellipsoidal bubble take part in the calculation of the rate of surface formation R_{sf} (Higbie, 1935). For oblate ellipsoidal bubbles (see Nedeltchev et al., 2006a, b):

$$R_{sf} = \pi \sqrt{\frac{l^2 + h^2}{2} - \frac{(l-h)^2}{8}} u_B \tag{21}$$

Equation (21) is needed for the calculation of the contact time t_c (Eq. 19) and thus the liquid–side mass transfer coefficient k_L (Eq. 20).
The number of bubbles N_B was deduced from the bubble residence time (aerated liquid height H divided by the bubble rise velocity u_B) and the bubble formation frequency f_B (Painmanakul et al., 2005; Nedeltchev et al., 2006a, b). The latter was expressed as volumetric flow rate Q_G divided by the bubble volume V_B (see Eqs. (3) and (6)). The interfacial area can be calculated as a function of bubble frequency f_B, bubble surface S_B, bubble rise velocity u_B and cross section (see Eq. (4)). Therefore, the theoretical k_La values for ellipsoidal bubbles can be calculated as a product of k_L value (estimated by means of Eqs. (5), (9), (10a-b), (20) and (21)) and a value (estimated by means of Eq. (4)).
The theoretical k_La values have to be multiplied with some correction factor f_c in order to match satisfactorily the experimental k_La values. Specifically, the accurate k_La values for ellipsoidal bubbles should be calculated by means of the following formula:

$$k_L a = f_c \sqrt{\frac{4 D_L R_{sf}}{\pi S_B}} \frac{f_B S_B}{A u_B} \tag{22}$$

The introduction of the correction factor f_c could be attributed to the fact that even when Eq. (19) is modified for oblate ellipsoidal bubbles it does not take into account the effect of the bubble wake and surface disturbances. Due to these supplementary effects on the mass transfer rate some additional term should be introduced.
Nedeltchev et al. (2006a) have illustrated that at pressures up to 1 MPa a good prediction of the experimental k_La values is achieved when the correction factor is expressed as a function only of the Eötvös number Eo:

$$f_c = 0.185 Eo^{0.737} \tag{23}$$

where

$$Eo = \frac{g(\rho_L - \rho_G) d_e^2}{\sigma_L} \tag{24}$$

The Eötvös number Eo represents the gravitational force–to–surface tension force ratio. As mentioned above, the bubble shape depends on the Eo value. Eqs. (23) and (24) show that as ρ_G increases and especially as bubble size reduces, Eo and thus f_c become lower.

The above–described theoretical method was applied to conduct a systematic comparison between predicted and experimental k_La results over a wide range of physicochemical properties, which are characteristic for gas–liquid systems. Both pure organic liquids and liquid mixtures as well as tap water were considered. In such a way, the capability of the correction method to predict the numerous experimental k_La data available in the literature was assessed. Following the introduction of an additional correction term accounting for the gas density effect, the predicted k_La values at high pressures were improved by as many as 18 % (in terms of the maximum relative error).

Volumetric liquid–phase mass transfer coefficients k_La measured in 18 organic liquids, 14 liquid mixtures and tap water at 293. 2 K (Tables 1 and 2) have been considered. Results for 1–butanol, ethanol (96 %), toluene, decalin and tap water were reported by Jordan and Schumpe (2001) for pressures P of 0.1, 0.2, 0.5, 1, 2 and 4 MPa, respectively. The k_La data in the other pure and organic liquids were measured at ambient pressure by Öztürk et al. (1987). These authors presented also some k_La data in tap water. All k_La data in the present approach refer to the dispersion volume.

The bubble column used by Jordan and Schumpe (2001) had an inner diameter of 0.1 m and a height of 2.4 m. Three different gas distributors were used: perforated plate, $19 \times Ø\ 1\times10^{-3}$ m (D1), single hole, $1 \times Ø\ 4.3\times10^{-3}$ m (D2) and single hole, $1 \times Ø\ 1\times10^{-3}$ m (D3). The clear liquid height was set at 1.3 m. Jordan and Schumpe (2001) measured their k_La values with a dynamic oxygen desorption technique. The oxygen desorption from the liquid was traced with an optical probe (MOPS, Comte, GmbH, Hannover, Germany) based on fluorescence extinction by oxygen. By dissolving the fluorophore in the liquid, rather than fixing it to the tip of the glass fiber, an instantaneous sensor response was achieved. It is worth noting that the D_L values for oxygen were either measured (Öztürk et al., 1987) or calculated by the correlation of Schumpe and Lühring (1990).

Öztürk et al. (1987) carried out their k_La experiments in a jacketed glass bubble column of 0.095 m in ID. The clear liquid height was set at 0.85 m. A single tube of $Ø\ 3\times10^{-3}$ m ID was used as the gas distributor (D4). Air, nitrogen, hydrogen or helium were employed as the gas phase.

The k_La values were measured by dynamic oxygen absorption or desorption methods. The oxygen fugacity in the liquids was measured with a polarographic oxygen electrode (WTW–EO 90) inserted horizontally at half the dispersion height. The electrode response time was 3 s in water and less in most organic liquids. For absorption runs, oxygen was desorbed by sparging nitrogen. After disengagement of all nitrogen bubbles, a preadjusted air flow was fed by switching two magnet valves, and the increase in oxygen fugacity was recorded. For desorption runs, oxygen–free inert gas (nitrogen, hydrogen or helium) was sparged into air–saturated liquid.

In the present work only k_La data obtained in the homogeneous flow regime of bubble column operation were analyzed. The upper boundary (so–called transitional gas velocity) of this flow regime was determined by the formulas of Reilly et al. (1994). According to the bubble shape diagrams presented by Clift et al. (1978) and Fan and Tsuchiya (1990) the bubbles formed under all operating conditions were oblate ellipsoidals.

By means of a nonlinear regressional routine applied to the experimental k_La data the following new correction factor was derived:

$$f_c = 0.124 Eo^{0.94}\left(\frac{\rho_G}{\rho_G^{ref}}\right)^{0.15} = 0.124\left(\frac{g(\rho_L-\rho_G)d_e^2}{\sigma_L}\right)^{0.94}\left(\frac{\rho_G}{1.2}\right)^{0.15} \quad (25)$$

where ρ_G^{ref} is the reference gas density (1.2 kg m^{-3} for air at ambient conditions: 293.2 K and 0.1 MPa). 263 experimental k_La values are fitted with an average relative error of 10.4 %. It is worth noting that this correction factor f_c combines the individual corrections of both k_L and a due to the ellipsoidal shape of bubbles. The average relative error without the gas density correction term is 14.9 %.

The dimensionless gas density ratio is the additional correction term that has not been reported hitherto. Its introduction is needed because the correlation of Wilkinson et al. (1994) was tested only up to 1.5 MPa. In our work we correlate k_La data at pressures of 2 and 4 MPa that could not be fitted without this term. Moreover, the correlations of Terasaka et al. (2004) have been derived under ambient pressure. To the best of our knowledge, these equations have not been validated under high pressure. It is worth noting that such a dimensionless gas density correction factor has been also used by Krishna (2000) for correcting his correlations for large bubble rise velocity and dense–phase gas holdup. The different correction factors reported in our previous papers (Nedeltchev et al., 2006a, b) are due to both lower number of liquids considered and lower operating pressures (up to 1 MPa).

Figs. 10a–10c show the parity plots of k_La values measured in four organic liquids aerated with three different distributors (D1, D2 and D3) at pressures up to 4 MPa.

It is clear that by means of the new correction factor (Eq. (25)) the k_La values can be predicted reasonably well (within ± 20 %). It is worth noting that the k_La values obtained in

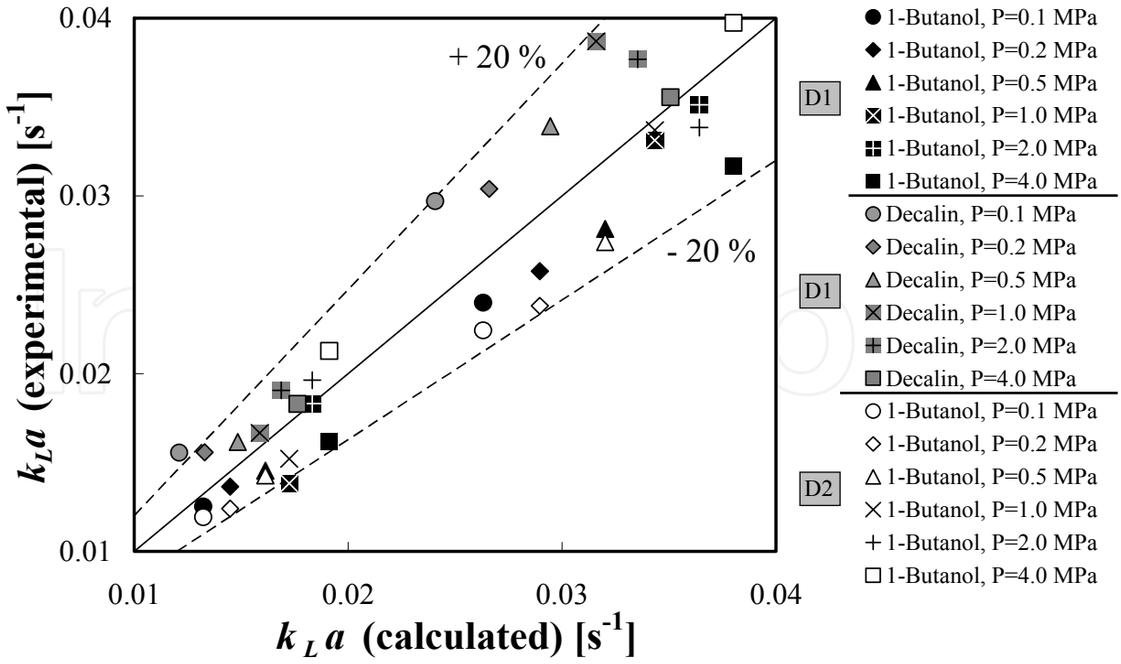

Fig. 10a. Parity plot of k_La values measured in 1–butanol and decalin at pressures up to 4 MPa (Gas distributors: D1 and D2)

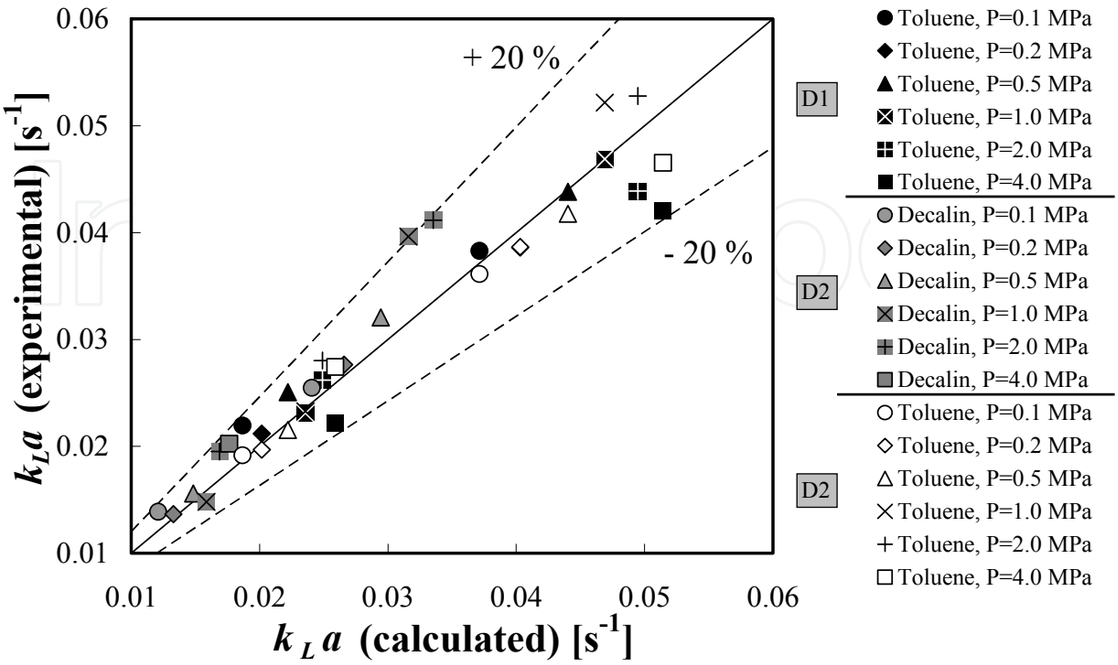

Fig. 10b. Parity plot of k_La values measured in toluene and decalin at pressures up to 4 MPa (Gas distributors: D1 and D2)

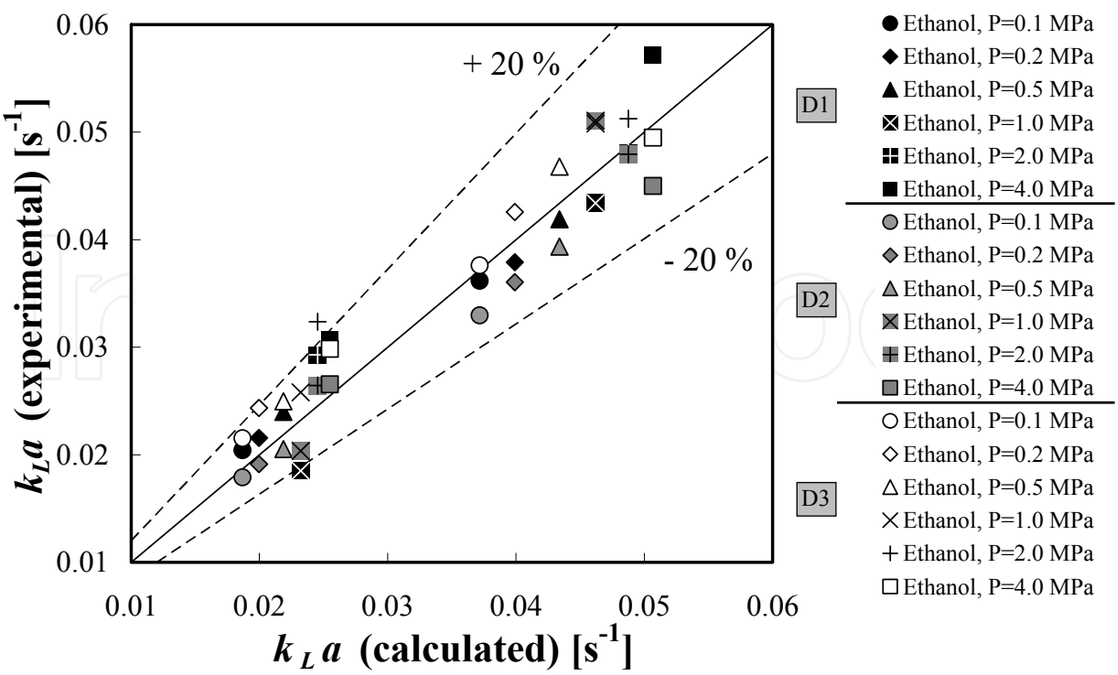

Fig. 10c. Parity plot of k_La values measured in ethanol (96 %) at pressures up to 4 MPa (Gas distributors: D1, D2 and D3)

tap water aerated with gas spargers D1 and D4 can also be predicted satisfactorily by means of Eq. (25). One of the merits of our work is the successful prediction of k_La data at very high pressure (up to 4 MPa). The presented theoretical approach predicts satisfactorily the k_La values measured by making use of four different gas distributors (D1–D4). It is known that the sparger has no substantial influence on both the gas holdup and mass transfer, provided that the diameter of the sparger holes is not too small (Wilkinson et al., 1994).

Fig. 11a exhibits that the correction method predicts satisfactorily the k_La values measured in 15 different organic liquids aerated with gas sparger D4 at ambient pressure. In the case of xylene and tetralin not only air (nitrogen) but also helium (He) and hydrogen were used. Ethanol (96 %) was also sparged with helium.

The new correction method applies not only to pure organic liquids but also to liquid mixtures. Fig. 11b shows that the predicted k_La values are in reasonable agreement with the experimental results. The keys for the different organic mixtures used are given in Table 2. All 14 organic mixtures were aerated with a gas sparger D4. As in some other parity plots, high k_La values tend to be overpredicted. This indicates the onset of coalescence at high gas velocity (flow regime transition). In Fig. 2b are included also predicted and experimental k_La values obtained in ethanol (96 %), toluene and 1–butanol aerated with helium (He) at different pressures by using different gas spargers (D2 and D3). These data demonstrate again that the developed theoretical approach along with the new correction factor (Eq. (25)) is valuable and capable of predicting numerous experimental k_La data.

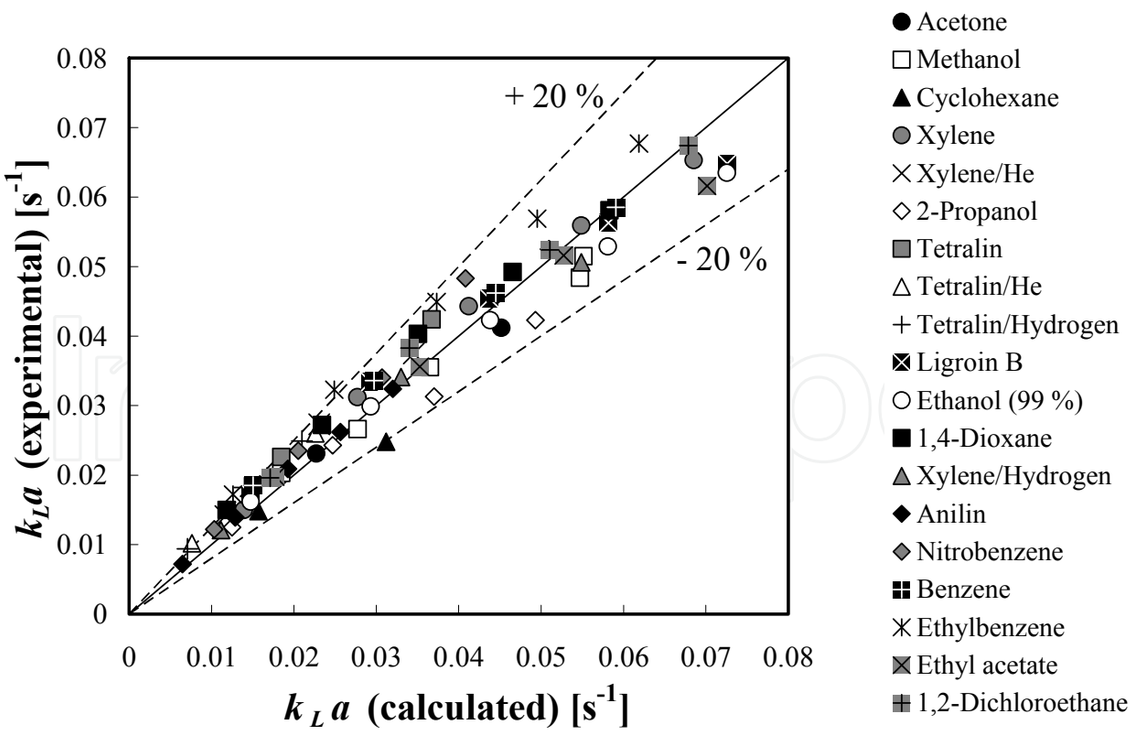

Fig. 11a. Parity plot of k_La values measured in 15 different organic liquids at ambient pressure (Gas distributor: D4)

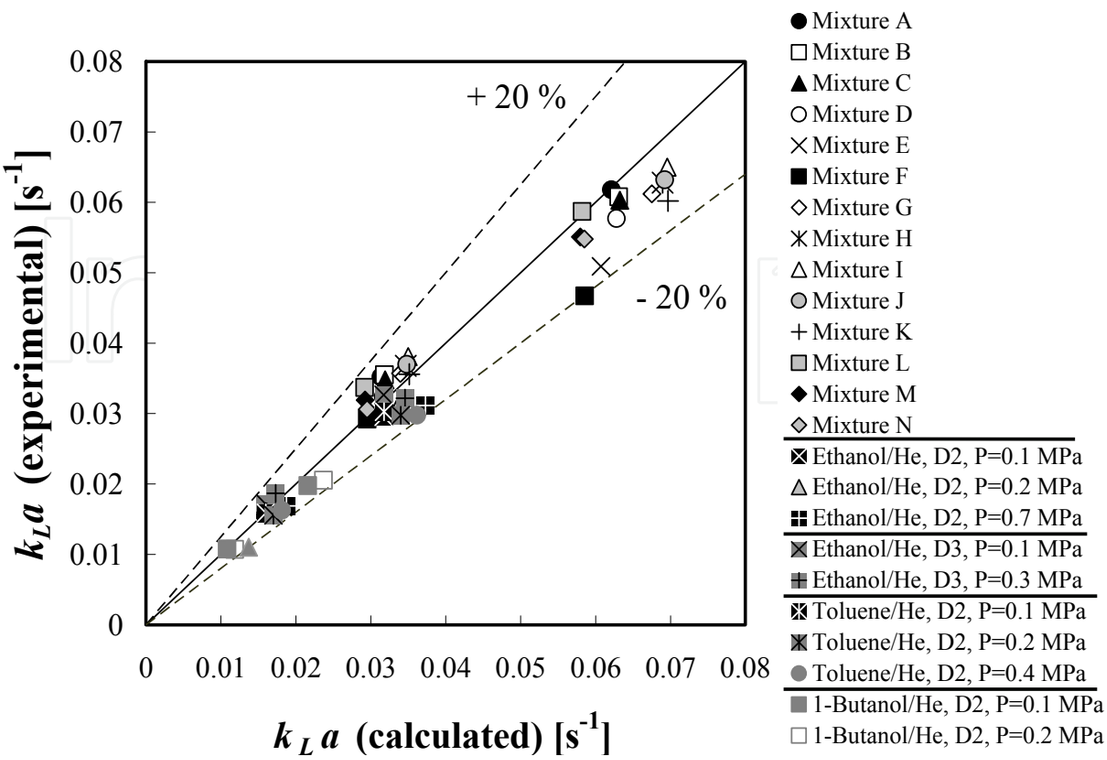

Fig. 11b. Parity plot of k_La values measured in 14 different liquid mixtures (P=0.1 MPa, sparger D4) as well as in ethanol, toluene and 1–butanol aerated with helium (He) at different pressures and gas spargers (D2, D3). The legend keys for the liquid mixtures are given in Table 2.

Fig. 12 shows the product $f_c(\rho_G/1.2)^{-0.15}$ (see Eq. (25)) as a function of Eo. This product increases with Eo for 13 organic liquids at ambient pressure. The trend holds also for different gases (air, nitrogen, helium and hydrogen). The $f_c(\rho_G/1.2)^{-0.15}$ values fall in the range of 0.3–1.1 which corresponds to Eo values from 2 to 10. It is worth noting that the f_c values for the liquids and operating conditions examined in this work are always lower than unity (0.3–0.8). In the case of the liquid mixtures specified in Table 2 the $f_c(\rho_G/1.2)^{-0.15}$ vs. Eo relationship follows the same trendline as the one shown in Fig. 12. For the sake of brevity this figure is omitted.

Nedeltchev et al. (2006a) have shown that the values of the correction factor (Eq. (23)) fall in line with the predictions of the correlation of Wellek et al. (1966) for the bubble aspect ratio E:

$$E - 1 = 0.163 Eo^{0.757} \tag{26}$$

where

$$E = \frac{l}{h} \tag{27}$$

This similarity holds also for Eq. (25). Figure 13 exhibits that the $f_c(\rho_G/1.2)^{-0.15}$ trendline at Eo≤5 is very close to the predictions of Eq. (26). Beyond this Eo value the values of the product $f_c(\rho_G/1.2)^{-0.15}$ become systematically higher than (E-1) values.

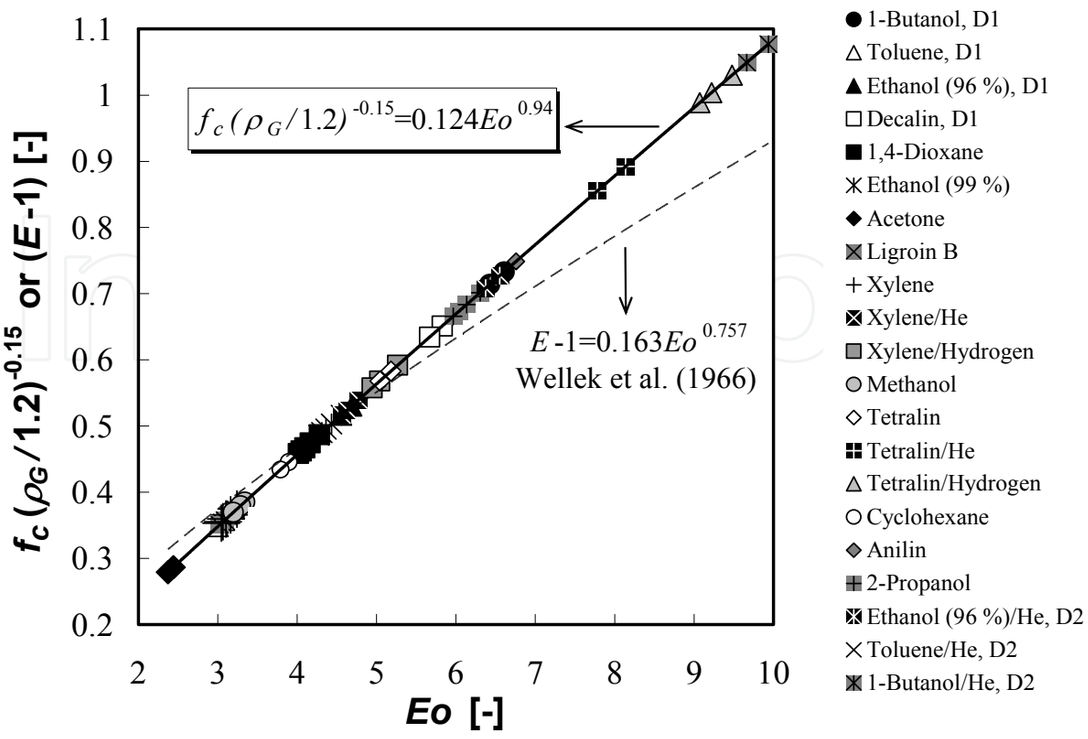

Fig. 12. Product $f_c(\rho_G/1.2)^{-0.15}$ as a function of the Eötvös number Eo for 13 different organic liquids at ambient pressure (Gas distributor: D4 unless otherwise mentioned)

It was found that the correction factors f_c gradually decrease with the increase of gas density ρ_G (operating pressure). As the superficial gas velocity u_G increases, a gradual f_c reduction is also observed. Both trends are illustrated for four organic liquids in Fig. 13. The decreasing f_c trends are explainable in terms of Eq. (25). The new correction factor f_c is primarily dependent on the Eötvös number Eo which involves the bubble equivalent diameter d_e. As u_G or ρ_G increases, the bubble size decreases (according to the correlation of Wilkinson et al. (1994)) leading to lower Eo and thus lower f_c (this trend is stronger than the effect of the gas density ratio).

Larger ellipsoidal bubbles are characterized with higher f_c values since larger wakes or vortices are formed behind them which enhance the mass transfer coefficient (see Lochiel and Calderbank, 1964; Miller, 1974) and thus the correction factor f_c becomes closer to unity. In addition, with larger ellipsoidal bubbles more surface disturbances occur which also enhance the mass transfer characteristics. Fan and Tsuchiya (1990) argue that larger ellipsoidal bubbles (larger Re_B) will have larger shedding frequency of vortex pairs from a bubble which will increase the mass transfer coefficient across the base of an ellipsoidal bubble and thus the overall liquid–phase mass transfer coefficient. It is worth noting that Eq. (20) is valid at very high bubble Reynolds numbers Re_B (Calderbank, 1967). It means that in the same liquid larger ellipsoidal bubbles will have higher Re_B and thus their correction factors f_c will be higher (closer to unity). The correction factor given in Eq. (25) supports this explanation. Lochiel and Calderbank (1964) have demonstrated that liquid drops (ethyl acetate drops in water and water drops in isobutanol) with larger diameter (higher Re_B) are characterized with higher correction factors.

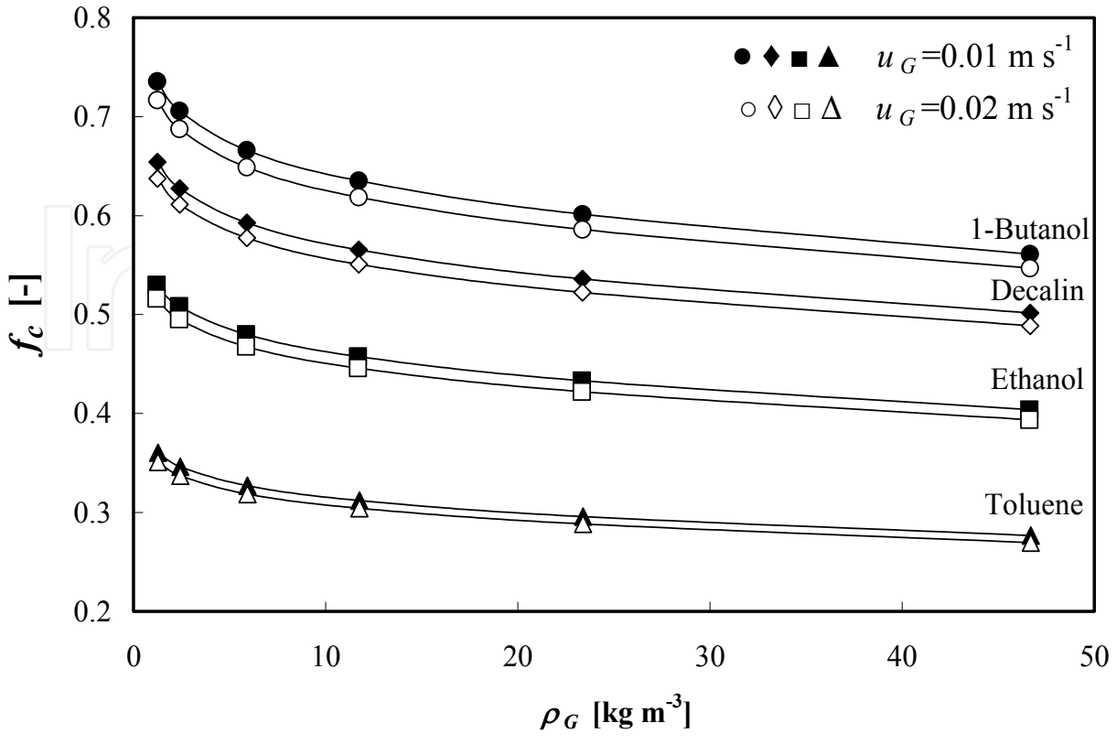

Fig. 13. Effects of both superficial gas velocity u_G and gas density ρ_G (operating pressure P) on the correction factor f_c. Gas distributor: D1–perforated plate, 19 × Ø 1×10^{-3} m, triangular pitch

The presented correction of the penetration theory is applicable in the homogeneous flow regime of bubble column operation. The upper boundary (so–called transitional gas velocity) of this flow regime was determined by the formulas of Reilly et al. (1994).

Only in the case of two other organic liquids, carbon tetrachloride and ethylene glycol (reported by Öztürk et al., 1987), the presented correction method was not capable of fitting the experimental k_La data satisfactorily. Table 1 shows that the correction method is applicable to organic liquids with densities ρ_L in the range of 714–1234 kg m^{-3} and viscosities μ_L in the range of 0.327–2.94×10^{-3} Pa s. Carbon tetrachloride has a higher liquid density (ρ_L=1593 kg m^{-3}), whereas ethylene glycol has a higher liquid viscosity (μ_L=19.94×10^{-3} Pa s).

In order to predict the k_La values (referred to liquid volume) at high temperature conditions, Nedeltchev et al. (2010) used another definition of the specific gas-liquid interfacial area a which is referred to unit liquid volume (see Lemoine et al., 2008):

$$a = \frac{6\varepsilon_G}{(1-\varepsilon_G)d_s} \tag{28}$$

It is worth noting that experimental gas holdups were used for calculating those interfacial areas. Two different elevated temperatures T (323 and 343 K) and three different operating pressures P (0.1, 0.2 and 0.5) were considered, respectively.

In the case of ellipsoidal bubbles, it is reasonable to assume that the correction factor f_c is proportional to the interphase drag coefficient C_D and the bubble eccentricity term (E−1) (taking into account the distortion from the perfect spherical shape). According to Olmos et

al. (2003) and Krishna and van Baten (2003) the drag coefficient C_D for ellipsoidal bubbles is a function of Eo:

$$C_D = \frac{2}{3}\sqrt{Eo} \tag{29}$$

The drag coefficient C_D accounts for the bubble-bubble interactions and bubble-induced turbulence. Raymond and Zieminski (1971) reported that there is a similarity in the behavior of the mass transfer coefficient and drag coefficient. The decrease of the mass transfer coefficient corresponds to an increase of the drag coefficient (due to friction drag for small bubbles or form drag for large bubbles) in the case of straight chain alcohols. According to Raymond and Zieminski (1971) the drag coefficient is proportional to the minor semi-axis of the ellipsoidal bubble. The authors reported also some dependence of the mass transfer coefficient on the bubble shape. Wellek et al. (1966) argue that the term (E−1) can be also correlated to the Eötvös number (see Eq. (26)).

Nedeltchev et al. (2010) expressed the correction factor f_c for prediction of k_La values (referred to liquid volume) as a product of both C_D and (E−1) as well as dimensionless temperature ratio:

$$f_c = B\, C_D (E-1)\left(\frac{T}{273.15}\right) \tag{30}$$

where B is proportionality constant.

The use of dimensionless temperature ratio is needed since the correlations for both C_D and (E−1) as well as Sauter-mean bubble size d_s (Eq. (15)), geometrical characteristics of the ellipsoidal bubbles (Eqs. (10a) and (10b)) and bubble rise velocity (Eq. (5)) were derived at ambient temperature and thus it is not certain whether they remain valid at elevated temperatures. It is worth noting that Cockx et al. (1995) introduced a correction term for the volumetric interfacial area which is also a function of the bubble eccentricity. Talvy et al. (2007a) have proven that the local bubble interfacial area is sensitive to the bubble shape. For bubble sizes above 3×10^{-3} m they have reported correction factors above 1.1. Talvy et al. (2007b) have shown that the ellipsoidal shape of the bubbles seems to be significant in estimation of the drag coefficient. When these correlations are improved and become applicable at various temperatures, then the dimensionless temperature ratio in Eq. (30) might become useless. The substitution of Eqs. (26) and (29) into Eq. (30) yields:

$$f_c = 0.109 B\, Eo^{1.257}\left(\frac{T}{273.15}\right) \tag{31}$$

By means of a non-linear regressional analysis applied to 167 k_La values (referred to liquid volume), the constant of proportionality B was estimated as 1.183. All k_La values were successfully fitted with an average relative error of 9.3 %.

The above-mentioned approach was also applied to slurry bubble columns operated in the homogeneous regime (Nedeltchev et al., 2007b). Six different liquid-solid systems (water/activated carbon, water/aluminium oxide, tetralin/aluminium oxide, 0.8 M sodium sulfate solution/kieselguhr (diatomaceous earth), ligroin (petroleum ether)/polyethylene and ligroin/polyvinylchloride) were considered. 85 experimental k_La values were fitted with a mean error of 19 %.

5. Conclusions

New approaches for the prediction of both gas holdups and volumetric liquid-phase mass transfer coefficients in gas-liquid and slurry bubble columns operated in the homogeneous regime have been developed. In these models the shape of the bubbles plays a major role. In the model for gas holdup prediction, the bubble surface and geometrical characteristics of the bubble (its length and height) are considered. In the model for k_La prediction the same parameters along with the circumference of the ellipsoidal bubbles (taking part in the rate of surface formation) are involved. In the process of evaluation of the mass transfer coefficient, it is made clear that Higbie's (1935) equation should be corrected due to the non-spherical shape of the bubbles. New correction factors were derived. The Eötvös number Eo plays a major role in them. Mass transfer coefficients at elevated temperatures can also be predicted by this approach.

As many as 23 organic liquids, 17 liquid mixtures and 6 liquid/solid systems were tested and the two major mass transfer parameters were predicted successfully.

6. Acknowledgment

Dr. Stoyan Nedeltchev expresses his gratitude to both DAAD and the Alexander von Humboldt Foundation (Germany) for the postdoctoral fellowships that made this research work possible. The financial support of the European Commission (7th Framework Programme, Grant Agreement No. 221832) for the continuation of this work is also gratefully acknowledged.

7. Nomenclature

A = cross–sectional area of the reactor	[m^2]
a = specific interfacial area (referred to dispersion volume)	[m^{-1}]
B = constant in Eqs. (30) and (31)	[–]
C_D = drag coefficient	[–]
D_c = column diameter	[m]
d_e = bubble equivalent diameter	[m]
D_L = molecular diffusivity	[$m^2 \cdot s^1$]
d_s = Sauter–mean bubble diameter	[m]
e , E = bubble eccentricity (9a) or (27)	[–]
Eo = Eötvös number, Eq. (24)	[–]
f_B = bubble formation frequency	[s^{-1}]
f_c = correction factor	[–]
g = gravitational acceleration	[$m \cdot s^{-2}$]
h = height of an ellipsoidal bubble	[m]
H = aerated liquid height	[m]
H_0 = clear liquid height	[m]
k_G =gas-phase mass transfer coefficient	[$m \cdot s^{-1}$]
k_Ga = volumetric gas-phase mass transfer coefficient	[s^{-1}]
k_L = liquid-phase mass transfer coefficient	[$m \cdot s^{-1}$]
k_La = volumetric liquid-phase mass transfer coefficient	[s^{-1}]
l = length (width) of an ellipsoidal bubble	[m]
Mo = Morton number, Eq. (14)	[–]

N_B = number of bubbles in the dispersion [–]
P = operating pressure [Pa]
ΔP = pressure difference between the readings of both lower (at 0 m) and upper (at 1.2 m) pressure transducers [Pa]
Q_G = gas flow rate [$m^3 \cdot s^{-1}$]
R_{sf} = rate of surface formation [$m^2 \cdot s^{-1}$]
Re = Reynolds number [–]
Re_B = bubble Reynolds number, Eq. (13) [–]
S_B = bubble surface [m^2]
Ta = Tadaki number, Eq. (12) [–]
T = operating temperature [K]
t_c = contact time [s]
u_B = bubble rise velocity [$m \cdot s^{-1}$]
u_G = superficial gas velocity [$m \cdot s^{-1}$]
u_{trans} = transition gas velocity [$m \cdot s^{-1}$]
V_B = bubble volume [m^3]
V_G = gas volume [m^3]
V_L = liquid volume [m^3]
V_{total} = dispersion volume [m^3]
We = Weber number [–]

8. Greek letters

ε_G = gas holdup [–]
μ_L = liquid viscosity [Pa·s]
ρ_G= gas density [$kg \cdot m^{-3}$]
ρ_G^{ref} = reference gas density (air at ambient conditions) [$kg \cdot m^{-3}$]
ρ_L = liquid density [$kg \cdot m^{-3}$]
σ_L = liquid surface tension [$N \cdot m^{-1}$]

9. References

Akita, K. & Yoshida, F. (1973). Gas Holdup and Volumetric Mass Transfer Coefficient in Bubble Columns, *Ind. Eng. Chem. Process Des. Dev.*, Vol. 12, 76-80

Akita, K. & Yoshida, F. (1974). Bubble Size, Interfacial Area and Liquid-Phase Mass Transfer Coefficient in Bubble Column, *Ind. Eng. Chem. Process Des. Dev.*, Vol. 13, 84-91

Akita, K. (1987a). Effect of Electrolyte on Mass Transfer Characteristics in Gas Bubble Column, *Kagaku Kogaku Ronbunshu,* Vol. 13, 166-172

Akita, K. (1987b). Effect of Trace Alcohol on Mass Transfer in Gas Bubble Column, *Kagaku Kogaku Ronbunshu,* Vol. 13, 181-187

Angelino, H. (1966). Hydrodynamique des grosses bulles dans les liquides visqueux, *Chem. Eng. Sci.,* Vol. 21, 541-550

Astarita, G. & Apuzzo, G. (1965). Motion of Gas Bubbles in Non-Newtonian Liquids, *AIChE J.*, Vol. 11, 815-820

Bach, H. F. & Pilhofer, T. (1978). Variation of Gas Holdup in Bubble Columns with Physical Properties of Liquids and Operating Parameters of Columns, *Ger. Chem. Eng.,* Vol. 1, 270

Baird, M. H. I. & Davidson J. F. (1962). Gas Absorption by Large Rising Bubbles, *Chem. Eng. Sci.,* Vol. 17, 87-93

Barnett, S. M.; Humphrey A. E. & Litt, M. (1966). Bubble Motion and Mass Transfer in Non-Newtonian Fluids, *AIChE J.,* Vol. 12, 253-259

Behkish, A.; Lemoine, R., Sehabiague, L., Oukaci, R. & Morsi, B. I. (2007). Gas Holdup and Bubble Size Behavior in a Large-Scale Slurry Bubble Column Reactor Operating with an Organic Liquid Under Elevated Pressures and Temperatures, *Chem. Eng. J.,* Vol. 128, 69-84

Botton, R.; Cosserat, D. & Charpentier, J. C. (1980). Mass Transfer in Bubble Columns Operating at High Gas Throughputs, *Chem. Eng. J.,* Vol. 20, 87-94

Calderbank, P. H. (1958). Physical Rate Process in Industrial Fermentation. Part I: The Interfacial Area in Gas-Liquid Contacting with Mechanical Agitation, *Trans. Inst. Chem. Engrs.,* Vol. 36, 443-463

Calderbank, P. H. & Moo-Young, M. B. (1961). The Continuous-Phase Heat and Mass-Transfer Properties of Dispersions, *Chem. Eng. Sci.,* Vol. 16, 39-54

Calderbank, P. H. & Lochiel A. C. (1964). Mass Transfer Coefficients, Velocities and Shapes of Carbon Dioxide Bubbles in Free Rise Through Distilled Water, *Chem. Eng. Sci.,* Vol. 19, 485-503

Calderbank, P. H. & Patra R. P. (1966). Mass Transfer in the Liquid Phase During the Formation of Bubbles, *Chem. Eng. Sci., Vol.* 21, 719-721

Calderbank, P. H. (1967). Gas Absorption from Bubbles. *Trans. Instn. Chem. Engrs.,* Vol. 45, CE209-CE233**.**

Calderbank, P. H.; Johnson, D. S. L. & Loudon, J. (1970). Mechanics and Mass Transfer of Single Bubbles in Free Rise Through Some Newtonian and Non-Newtonian Liquids, *Chem. Eng. Sci.,* Vol. 25, 235-256

Chen, R. C.; Reese, J. & Fan, L.-S. (1994). Flow Structure in a Three-Dimensional Bubble Column and Three-Phase Fluidized Bed, *AIChE J.,* Vol. 40, 1093-1104

Cho, J. S. & Wakao, N. (1988). Determination of Liquid-Side and Gas-Side Volumetric Mass Transfer Coefficients in a Bubble Column, *J. Chem. Eng. Japan,* Vol. 21, 576-581

Clift, R.; Grace, J. R. & Weber, M. (1978). *Bubbles, Drops and Particles*, Academic Press, New York, U. S. A.

Cockx, A.; Roustan, M., Line, A. & Hebrard, G. (1995). Modelling of Mass Transfer Coefficient k_L in Bubble Columns, *Trans. Instn. Chem. Engrs.,* Vol. 73(A), 617-631

Davenport, W. G.; Richardson, F. D. & Bradshaw, A. V. (1967). Spherical Cap Bubbles in Low Density Liquids, *Chem. Eng. Sci.,* Vol. 22, 1221-1235

Davidson, J. F. & Harrison, D. (1963). *Fluidised Particles*, Cambridge University Press, UK.

Davies, R. M. & Taylor, G. I. (1950). *Proc. Roy. Soc.,* Vol. A200, 375

Deckwer, W.-D. (1980). On the Mechanism of Heat Transfer in Bubble Column Reactors. *Chem. Eng. Sci.*, Vol. 35, 1341-1346.

Deckwer, W.-D. (1992). *Bubble Column Reactors*, John Wiley and Sons, Chichester, UK.

Fan, L.-S. & Tsuchiya, K. (1990). *Bubble Wake Dynamics in Liquids and Liquid–Solid Suspensions*, Butterworth–Heinemann Series in Chemical Engineering, Stoneham, U.S.A.

Fukuma, M.; Muroyama, K. & Yasunishi, A. (1987a). Properties of Bubble Swarm in a Slurry Bubble Column, *J. Chem. Eng. Japan,* Vol. 20, 28-33

Fukuma, M.; Muroyama, K. & Yasunishi, A. (1987b). Specific Gas-Liquid Interfacial Area and Liquid-Phase Mass Transfer Coefficient in a Slurry Bubble Column, *J. Chem. Eng. Japan,* Vol. 20, 321-324

Gandhi, A. B.; Joshi, J. B., Jayaraman, V. K. & Kulkarni, B. D. (2007). Development of Support Vector Regression (SVR)-Based Correlation for Prediction of Overall Gas Hold-Up in Bubble Column Reactors for Various Gas–Liquid Systems, *Chem. Eng. Sci.* Vol. 62, 7078-7089

Godbole, S. P.; Honath M. F. & Shah, Y. T. (1982). Holdup Structure in Highly Viscous Newtonian and Non-Newtonian Liquids in Bubble Columns, *Chem. Eng. Commun.*, Vol. 16, 119-134

Godbole, S. P.; Schumpe, A., Shah, Y. T. & Carr, N. L. (1984). Hydrodynamics and Mass Transfer in Non-Newtonian Solutions in a Bubble Column, *AIChE J.,* Vol. 30, 213-220

Griffith, R. M. (1960). Mass Transfer from Drops and Bubbles, *Chem. Eng. Sci.,* Vol. 12, 198-213

Grund, G.; Schumpe, A. & Deckwer, W.-D. (1992). Gas-Liquid Mass Transfer in a Bubble Column with Organic Liquids, *Chem. Eng. Sci.,* Vol. 47, 3509-3516

Hammer, H.; Schrag, H., Hektor, K., Schönau, K., Küsters, W., Soemarno, A., Sahabi U. & Napp, W. (1984). New Subfunctions on Hydrodynamics, Heat and Mass Transfer for Gas/Liquid and Gas/Liquid/Solid Chemical and Biochemical Reactors, *Front. Chem. Reac. Eng.*, 464-474

Hammerton, D. & Garner, F. H. (1954). *Trans. Instn. Chem. Engrs.,* Vol. 32, S18

Hayashi, T.; Koide K. & Sato, T. (1975). Bubbles Generated from Porous Plate in Organic Solutions and Aqueous Solutions of Organic Substances, *J. Chem. Eng. Japan,* Vol. 8, 16-20

Higbie, R. (1935). The Rate of Absorption of Pure Gas into a Still Liquid During Short Periods of Exposure, *Trans. AIChE,* Vol. 31, 365-389

Hikita, H.; Asai, S., Tanigawa, K., Segawa, K. & Kitao, M. (1980). Gas Holdup in Bubble Columns, *Chem. Eng. J.,* Vol. 20, 59-67

Hikita, H.; Asai, S., Tanigawa, K., Segawa, K. & Kitao, M. (1981). The Volumetric Liquid-Phase Mass Transfer Coefficient in Bubble Columns, *Chem. Eng. J.,* Vol. 22, 61

Hughmark, G. A. (1967). Holdup and Mass Transfer in Bubble Columns, *Ind. Eng. Chem. Process Des. Dev.,* Vol. 6, 218-220

Idogawa, K.; Ikeda, K., Fukuda, T. & Morooka, S. (1985a). Behavior of Bubbles in a Bubble Column under High Pressure for Air-Water System, *Kagaku Kogaku Ronbunshu,* Vol. 11, 253-258

Idogawa, K.; Ikeda K., Fukuda, T. & Morooka, S. (1985b). Effects of Gas and Liquid Properties on the Behavior of Bubbles in a Bubble Column under High Pressure, *Kagaku Kogaku Ronbunshu*, Vol. 11, 432-437

Idogawa, K.; Ikeda, K., Fukuda, T. & Morooka, S. (1987). Effect of Gas and Liquid Properties on the Behaviour of Bubbles in a Column Under High Pressure, *Intern. Chem. Eng.*, Vol. 27, 93-99

Jiang, P.; Lin, T.-J., Luo, X. & Fan, L.-S. (1995). Flow Visualization of High Pressure (21 MPa) Bubble Columns: Bubble Characteristics, *Trans. Inst. Chem. Eng.,* Vol. 73, 269-274

Jordan, U. & Schumpe, A. (2001). The Gas Density Effect on Mass Transfer in Bubble Columns with Organic Liquids, *Chem. Eng. Sci.,* Vol. 56, 6267-6272

Kastanek, F. (1977). The Volume Mass Transfer Coefficient in a Bubble Bed Column, *Collect. Czech. Chem. Commun.,* Vol. 42, 2491-2497

Kastanek, F.; J. Zahradnik, Kratochvil J. & Cermak, J. (1993). *Chemical Reactors for Gas-Liquid Systems*, Ellis Horwood, Chichester, West Sussex, UK

Kawase, Y. & Moo-Young, M. (1986). Influence of Non-Newtonian Flow Behaviour on Mass Transfer in Bubble Columns with and without Draft Tubes, *Chem. Eng. Commun.,* Vol. 40, 67-83

Kawase, Y.; Halard, B. & Moo-Young, M. (1987). Theoretical Prediction of Volumetric Mass Transfer Coefficients in Bubble Columns for Newtonian and Non-Newtonian Fluids, *Chem. Eng. Sci.,* Vol. 42, 1609-1617

Kelkar, B. G.; Godbole, S. P., Honath, M. F., Shah, Y. T., Carr, N. L. & Deckwer, W.-D. (1983). Effect of Addition of Alcohols on Gas Holdup and Backmixing in Bubble Columns, *AIChE J.*, Vol. 29, 361-369

Khare, A. S. & Joshi, J. B. (1990). Effect of Fine Particles on Gas Holdup in Three-Phase Sparged Reactors, *Chem. Eng. J.,* Vol. 44, 11

Kiambi, S. L.; Duquenne, A. M., Bascoul, A. & Delmas, H. (2001). Measurements of Local Interfacial Area: Application of Bi-Optical Fibre Technique, *Chem. Eng. Sci.,* Vol. 56, 6447-6453

Koide, K.; Hirahara, T. & Kubota, H. (1966). Average Bubble Diameter, Slip Velocity and Gas Holdup of Bubble Swarms, *Kagaku Kogaku*, Vol. 30, 712-718

Koide, K.; Kato, S., Tanaka, Y. & Kubota, H. (1968). Bubbles Generated from Porous Plate, *J. Chem. Eng. Japan,* Vol. 1, 51-56

Koide, K.; Takazawa, A., Komura M. & Matsunaga, H. (1984). Gas Holdup and Volumetric Liquid-Phase Mass Transfer Coefficient in Solid-Suspended Bubble Columns, *J. Chem. Eng. Japan,* Vol. 17, 459-466

Koide, K. (1996). Design Parameters of Bubble Column Reactors With and Without Solid Suspensions, *J. Chem. Eng. Japan,* Vol. 29, 745-759

Kolmogoroff, A. N. (1941). *Dokl. Akad. Nauk SSSR,* Vol. 30, 301

Krishna, R.; Wilkinson, P. M. & Van Dierendonck, L. L. (1991). A Model for Gas Holdup in Bubble Columns Incorporating the Influence of Gas Density on Flow Regime Transitions, *Chem. Eng. Sci*., Vol. 46, 2491-2496

Krishna, R. (2000). A Scale-Up Strategy for a Commercial Scale Bubble Column Slurry Reactor for Fischer-Tropsch Synthesis, Oil and Gas Science and Techn.-Rev. IFP, Vol. 55, 359-393

Krishna, R. & van Baten, J. M. (2003). Mass Transfer in Bubble Columns, Catalysis Today 79-80, 67-75

Kulkarni, A.; Shah, Y. T. & Kelkar, B. G. (1987). Gas Holdup in Bubble Column with Surface-Active Agents: a Theoretical Model, *AIChE J.*, Vol. 33, 690-693

Kumar, A.; Degaleesan, T. T., Laddha, G. S. & Hoelscher, H. E. (1976). Bubble Swarm Characteristics in Bubble Columns, *Can. J. Chem. Eng.,* Vol. 54, 503-508

Lemoine, R.; Behkish, A., Sehabiague, L., Heintz, Y. J., Oukaci, R. & Morsi, B. I. (2008). An Algorithm for Predicting the Hydrodynamic and Mass Transfer Parameters in Bubble Column and Slurry Bubble Column Reactors, Fuel Proc. Technol., Vol. 89, 322-343

Leonard, J. H. & Houghton, G. (1961). *Nature* (London), Vol. 190, 687

Leonard, J. H. & Houghton, G. (1963). Mass Transfer and Velocity of Rise Phenomena for Single Bubbles, *Chem. Eng. Sci.,* Vol. 18, 133-142

Lochiel, C. & Calderbank, P. H. (1964). Mass Transfer in the Continuous Phase Around Axisymmetric Bodies of Revolution, *Chem. Eng. Sci.*, Vol. 19, 471-484

Lucas, D.; Prasser, H.-M. & Manera, A. (2005). Influence of the Lift Force on the Stability of a Bubble Column, Chem. Eng. Sci., Vol. 60, 3609-3619

Marrucci, G. (1965). Rising Velocity of a Swarm of Spherical Bubbles, *Ind. Eng. Chem. Fund.,* Vol. 4, 224-225

Mendelson, H. D. (1967). The Prediction of Bubble Terminal Velocities from Wave Theory, *AIChE J.,* Vol. 13, 250-253

Merchuk, J. C. & Ben-Zvi, S. (1992). A Novel Approach to the Correlation of Mass Transfer Rates in Bubble Columns with Non-Newtonian Liquids, *Chem. Eng. Sci.,* Vol. 47, 3517-3523

Metha, V. D. & Sharma, M. M. (1966). Effect of Diffusivity on Gas-Side Mass Transfer Coefficient, *Chem. Eng. Sci.,* Vol. 21, 361-365

Miller, D. N. (1974). Scale-Up of Agitated Vessels Gas-Liquid Mass Transfer, *AIChE J.,* Vol. 20, 445-453

Miyahara, T. & Hayashi, T. (1995). Size of Bubbles Generated from Perforated Plates in Non-Newtonian Liquids, *J. Chem. Eng. Japan,* Vol. 28, 596-600

Muller, F. L. & Davidson J. F. (1992). On the Contribution of Small Bubbles to Mass Transfer in Bubble Columns Containing Highly Viscous Liquids, *Chem. Eng. Sci.,* Vol. 47, 3525-3532

Nakanoh, M. & Yoshida, F. (1980). Gas Absorption by Newtonian and Non-Newtonian Liquids in a Bubble Column, *Ind. Eng. Chem. Process Des. Dev.,* Vol. 19, 190-195

Nedeltchev, S.; Jordan, U. & Schumpe, A. (2006a). Correction of the Penetration Theory Applied to the Prediction of k_La in a Bubble Column with Organic Liquids, *Chem. Eng. Tech.*, Vol. 29, 1113-1117

Nedeltchev, S.; Jordan, U. & Schumpe, A. (2006b). A New Correction Factor for Theoretical Prediction of Mass Transfer Coefficients in Bubble Columns, *J. Chem. Eng. Japan*, Vol. 39, 1237-1242

Nedeltchev, S.; Jordan, U. & Schumpe, A. (2007a). Correction of the Penetration Theory Based On Mass-Transfer Data from Bubble Columns Operated in the Homogeneous Regime Under High Pressure, *Chem. Eng. Sci.*, Vol. 62, 6263-6273

Nedeltchev, S. & Schumpe, A. (2007b). Theoretical Prediction of Mass Transfer Coefficients in a Slurry Bubble Column Operated in the Homogeneous Regime, *Chem. & Biochem. Eng. Quarterly*, Vol. 21, 327-334

Nedeltchev, S. & Schumpe, A. (2008). A New Approach for the Prediction of Gas Holdup in Bubble Columns Operated Under Various Pressures in the Homogeneous Regime, *J. Chem. Eng. Japan,* Vol. 41, 744-755

Nedeltchev, S.; Jordan U. & Schumpe, A. (2010). Semi-Theoretical Prediction of Volumetric Mass Transfer Coefficients in Bubble Columns with Organic Liquids at Ambient and Elevated Temperatures, *Can. J. Chem. Eng.,* Vol. 88, 523-532

Olmos, E., Gentric, C. & Midoux, N. (2003). Numerical Description of Flow Regime Transitions in Bubble Column Reactors by a Multiple Gas Phase Model, *Chem. Eng. Sci.*, Vol. 58, 2113-2121

Otake, T.; Tone, S., Nakao, K. & Mitsuhashi, Y. (1977). Coalescence and Breakup of Bubbles in Liquids, *Chem. Eng. Sci.*, Vol. 32, 377-383

Öztürk, S; Schumpe, A. & Deckwer, W.-D. (1987). Organic Liquids in a Bubble Column: Holdups and Mass Transfer Coefficients, *AIChE J.,* Vol. 33, 1473-1480

Painmanakul, P.; Loubière, K., Hébrard, G., Mietton-Peuchot, M. & Roustan, M. (2005). Effect of Surfactants on Liquid–Side Mass Transfer Coefficients, *Chem. Eng. Sci.*, Vol. 60, 6480-6491

Pošarac, D. & Tekić, M. N. (1987). Gas Holdup and Volumetric Mass Transfer Coefficient in Bubble Columns with Dilute Alcohol Solutions, *AIChE J.*, Vol. 33, 497–499

Raymond, D. R. & Zieminski, S. A. (1971). Mass Transfer and Drag Coefficients of Bubbles Rising in Dilute Aqueous Solutions. *AIChE J.*, Vol. 17, 57-65

Redfield, J. A. & Houghton, G. (1965). Mass Transfer and Drag Coefficients for Single Bubbles at Reynolds Numbers of 0.02-5000, *Chem. Eng. Sci., Vol.* 20, 131-139

Reilly, I. G.; Scott, D. S., de Bruijn, T. J. W., Jain, A. K. & Piskorz, J. (1986). Correlation for Gas Holdup in Turbulent Coalescing Bubble Columns, *Can. J. Chem. Eng.* 64, 705-717

Reilly, I. G.; Scott, D. S., De Bruijn, T. J. W. & MacIntyre, D. (1994). The Role of Gas Phase Momentum in Determining Gas Holdup and Hydrodynamic Flow Regimes in Bubble Column Operations, *Can. J. Chem. Eng.*, Vol. 72, 3-12

Sada, E.; Kumazawa, H., Lee, E. & Fujiwara, N. (1985). Gas-Liquid Mass Transfer Characteristics in Bubble Columns with Suspended Sparingly Soluble Fine Particles, *Ind. Eng. Chem. Process Des. Dev.,* Vol. 24, 255-261

Sada, E.; Kumazawa, H., Lee, E. & Iguchi, T. (1986). Gas Holdup and Mass Transfer Characteristics in a Three-Phase Bubble Column, *Ind. Eng. Chem. Process Des. Dev.*, Vol. 25, 472-476

Salvacion, J. L.; Murayama, M., Ohtaguchi, K. & Koide, K. (1995). Effects of Alcohols on Gas Holdup and Volumetric Liquid-Phase Mass Transfer Coefficient in Gel-Particle Suspended Bubble Column," *J. Chem. Eng. Japan,* Vol. 28, 434-442

Sauer, T. & Hempel, D.-C. (1987). Fluid Dynamics and Mass Transfer in a Bubble Column with Suspended Particles, *Chem. Eng. Technol., Vol.* 10, 180-189

Schumpe, A. & Deckwer, W.-D. (1987). Viscous Media in Tower Bioreactors: Hydrodynamic Characteristics and Mass Transfer Properties, *Bioprocess Eng.,* Vol. 2, 79-94

Schumpe, A.; Saxena, A. K. & Fang, L. K. (1987). Gas/Liquid Mass Transfer in a Slurry Bubble Column, *Chem. Eng. Sci.*, Vol. 42, 1787-1796

Schumpe, A. & Lühring, P. (1990). Oxygen Diffusivities in Organic Liquids at 293.2 K, J. Chem. and Eng. Data, Vol. 35, 24-25

Schügerl, K.; Lucke, J. & Oels, U. (1977). Bubble Column Bioreactors, *Adv. Biochem. Eng.*, Vol. 7, 1-84

Shah, Y. T.; Kelkar, B. G. & Deckwer, W.-D. (1982). Design Parameters Estimation for Bubble Column Reactors, *AIChE J.*, Vol. 28, 353-379

Suh, I.-S.; Schumpe, A., Deckwer, W.-D. & Kulicke, W.-M. (1991). Gas-Liquid Mass Transfer in the Bubble Column with Viscoelastic Liquid, *Can. J. Chem. Eng.*, Vol. 69, 506-512

Sun, Y. & Furusaki, S. (1989). Effect of Intraparticle Diffusion on the Determination of the Gas-Liquid Volumetric Oxygen Transfer Coefficient in a Three-Phase Fluidized Bed Containing Porous Particles, *J. Chem. Eng. Japan*, Vol. 22, 556-559

Syeda, S. R.; Afacan, A. & Chuang, K. T. (2002). Prediction of Gas Hold–Up in a Bubble Column Filled with Pure and Binary Liquids, *Can. J. Chem. Eng*., Vol. 80, 44-50

Tadaki, T. & Maeda, S. (1961). On Shape and Velocity of Single Air Bubble Rising in Various Liquids, *Kagaku Kogaku*, Vol. 25, 254-264

Tadaki, T. & Maeda, S. (1963). The Size of Bubbles from Single Orifice, *Kagaku Kogaku,* Vol. 27, 147-155

Talvy, S.; Cockx, A. & Line, A. (2007a). Modeling of Oxygen Mass Transfer in a Gas–Liquid Airlift Reactor, AIChE J., Vol. 53, 316-326

Talvy, S.; Cockx, A. & Line, A. (2007b). Modeling Hydrodynamics of Gas–Liquid Airlift Reactor," AIChE J., Vol. 53, 335-353

Terasaka, K.; Inoue, Y., Kakizaki, M. & Niwa, M. (2004). Simultaneous Measurement of 3–Dimensional Shape and Behavior of Single Bubble in Liquid Using Laser Sensors, *J. Chem. Eng. Japan*, Vol. 37, 921-926

Timson, W. J. & Dunn, C. J. (1960). Mechanism of Gas Absorption from Bubbles Under Shear, *Ind. & Eng. Chem*., Vol. 52, 799-802

Tsuchiya, K. & Nakanishi, O. (1992). Gas Holdup Behavior in a Tall Bubble Column with Perforated Plate Distributors, *Chem. Eng. Sci.,* Vol. 47, 3347-3354

Ueyama, K.; Morooka, S., Koide, K., Kaji, H. & Miyauchi, T. (1980). Behavior of Gas Bubbles in Bubble Columns, *Ind. Eng. Chem. Process Des. Dev.,* Vol. 19, 592-599

Wellek, R. M., Agrawal, A. K. & Skelland, A. H. P. (1966). Shape of Liquid Drops Moving in Liquid Media, AIChE J., Vol. 12, 854-862

Wilkinson, P. M. & van Dierendonck, L. L. (1990). Pressure and Gas Density Effects on Bubble Breakup and Gas Holdup in Bubble Columns, *Chem. Eng. Sci.,* Vol. 45, 2309-2315

Wilkinson, P. M.; Spek A. P. & Van Dierendonck, L. L. (1992). Design Parameters Estimation for Scale-Up of High-Pressure Bubble Columns, *AIChE J.,* Vol. 38, 544-554

Wilkinson, P. M.; Haringa, H. & Van Dierendonck, L. L. (1994). Mass Transfer and Bubble Size in a Bubble Column under Pressure, *Chem. Eng. Sci.,* Vol. 49, 1417-1427

Yamashita, F.; Mori Y. & Fujita, S. (1979). Sizes and Size Distributions of Bubbles in a Bubble Column, *J. Chem. Eng. Japan,* Vol. 12, 5-9

Yasunishi, A.; Fukuma, M. & Muroyama, K. (1986). Hydrodynamics and Gas-Liquid Mass Transfer Coefficient in a Slurry Bubble Column with High Solid Content, *Kagaku Kogaku Ronbunshu,* Vol. 12, 420-426

Zieminski, S. A. & Raymond, D. R. (1968). Experimental Study of the Behaviour of Single Bubbles, *Chem. Eng. Sci.,* Vol. 23, 17-28

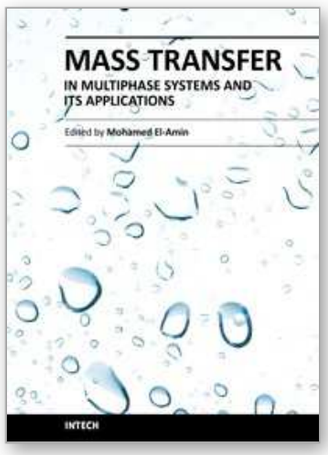

Mass Transfer in Multiphase Systems and its Applications
Edited by Prof. Mohamed El-Amin

ISBN 978-953-307-215-9
Hard cover, 780 pages
Publisher InTech
Published online 11, February, 2011
Published in print edition February, 2011

This book covers a number of developing topics in mass transfer processes in multiphase systems for a variety of applications. The book effectively blends theoretical, numerical, modeling and experimental aspects of mass transfer in multiphase systems that are usually encountered in many research areas such as chemical, reactor, environmental and petroleum engineering. From biological and chemical reactors to paper and wood industry and all the way to thin film, the 31 chapters of this book serve as an important reference for any researcher or engineer working in the field of mass transfer and related topics.

InTech Europe
University Campus STeP Ri
Slavka Krautzeka 83/A
51000 Rijeka, Croatia
Phone: +385 (51) 770 447
Fax: +385 (51) 686 166
www.intechopen.com

InTech China
Unit 405, Office Block, Hotel Equatorial Shanghai
No.65, Yan An Road (West), Shanghai, 200040, China
中国上海市延安西路65号上海国际贵都大饭店办公楼405单元
Phone: +86-21-62489820
Fax: +86-21-62489821

IntechOpen